Abstract

Wave propagation is described by the wave equation, or in the time-periodic case, by the Helmholtz equation. For problems with small wavelengths, high order discretizations must be used to resolve the solution. Two different techniques for finding compact finite difference schemes of high order are studied and compared. The first approach is Numerov's idea of using the equation to transfer higher derivatives to lower order ones for the Helmholtz equation, or, for the wave equation, from time to space. The second principle is the method of deferred correction, where a lower order approximation is used for error correction.

For the time-independent Helmholtz problem, sharp estimates for the error is derived, in order to compare the arithmetic complexity for both approaches with a non-compact scheme. The characteristics of the errors for fourth order as well as sixth order accuracy are demonstrated and the advantages and disadvantages of the methods are discussed.

A time compact, Numerov-type, fourth order method and a fourth order method using deferred correction in time are studied for the wave equation. Schemes are derived for both the second order formulation of the equation, and for the system in first order form. Stability properties are analyzed and numerical experiments have been performed, for both constant and variable coefficients in the equations. For the first order formulation, a staggered grid is used.

Keywords: Helmholtz equation, wave equation, finite difference method, compact scheme, deferred correction.

Acknowledgments

I would like to thank my supervisor Prof. Bertil Gustafsson for all his work and support. I am also grateful to Dr. Kurt Otto and Dr. Leif Abrahamsson for sharing some of their deep knowledge with me, and to my husband Magnus for his help.

Chapter 1

Introduction

Wave propagation problems appear in many different areas in applied mathematics, such as aero- or underwater acoustics [17] or electromagnetics [3]. The motion of waves is described by the wave equation, or in the time-harmonic case, the Helmholtz equation. Numerical methods for these have been studied extensively for decades, but real-world applications where the wavelengths of the problems are very much smaller than the computational area give prohibitively large discretized problems, if the wave oscillations are to be properly resolved. Therefore, with the objective to develop efficient finite difference solvers for the wave equation or the Helmholtz equation, we will present a survey of different approaches to derive higher order methods.

1 Governing equations

We now state the equations we wish to solve. They are the wave equation in second order form (1.1), the equivalent formulation as a first order system (1.2), and the Helmholtz equation (1.5).

1.1 The wave equation

The wave propagation is found by solving

$$\frac{1}{a(\boldsymbol{x})}\frac{\partial^2\phi}{\partial t^2} = \nabla\cdot\big(b(\boldsymbol{x})\,\nabla\phi\big) + \tilde{\tilde{F}}(\boldsymbol{x},t) \tag{1.1}$$

together with appropriate boundary conditions. With the new variables

$$\begin{aligned}\varphi(\boldsymbol{x},t) &= \frac{\partial\phi}{\partial t} + \tilde{F}(\boldsymbol{x},t) \qquad \text{and}\\ \boldsymbol{\psi}(\boldsymbol{x},t) &= b(\boldsymbol{x})\,\nabla\phi + \tilde{\boldsymbol{G}}(\boldsymbol{x},t)\,,\end{aligned}$$

can (1.1) be rewritten as

$$
\begin{aligned}
\varphi_t &= a\,(\boldsymbol{x})\,\nabla\cdot\boldsymbol{\psi} + F(\boldsymbol{x},t)\,,\\
\boldsymbol{\psi}_t &= b(\boldsymbol{x})\nabla\varphi + \boldsymbol{G}(\boldsymbol{x},t)\,,
\end{aligned}
\tag{1.2}
$$

with F and $\boldsymbol{G}$ determined from $\tilde{\tilde{F}}$, $\tilde{F}$ and $\tilde{\boldsymbol{G}}$. Also φ (and higher order time derivatives of ϕ) satisfies a wave equation in second order form like (1.1).

As a first example of an area where the wave equation is of importance, we consider sound propagation in a fluid [2]. For a fluid with negligible viscosity, the flow is described by the Euler equations, relating the velocity field $\boldsymbol{u}(\boldsymbol{x},t)$, the density $\rho(\boldsymbol{x})$ and the pressure $p(\boldsymbol{x},t)$. Expressed with the summation convention, they are

$$
\begin{aligned}
&\frac{\partial\rho}{\partial t} + \frac{\partial}{\partial x_j}(\rho u_j) = 0\,,\\
&\frac{\partial u_i}{\partial t} + u_j\frac{\partial u_i}{\partial x_j} + \rho^{-1}\frac{\partial p}{\partial x_i} = 0\,.
\end{aligned}
$$

To close the system, we use the equation of state that relates the pressure to the density and the entropy:

$$p = p(\rho, S)\,,$$

For adiabatic flow,

$$\frac{\partial S}{\partial t} + \boldsymbol{u}\cdot\nabla S = 0\,,$$

giving

$$\frac{\partial p}{\partial t} + \boldsymbol{u}\cdot\nabla p = c^2\frac{\partial\rho}{\partial t} + c^2\boldsymbol{u}\cdot\nabla\rho\,,$$

with

$$c^2(\boldsymbol{x}) = \left.\frac{\partial p}{\partial\rho}\right|_S > 0 \text{ for all } \boldsymbol{x}$$

We now consider one-dimensional flow, and use the equation of state in the conservation equations to find the reduced equations:

$$
\begin{aligned}
&p_t + up_x + c^2\rho u_x = 0\,,\\
&\rho(u_t + uu_x) + p_x = 0\,.
\end{aligned}
$$

To show how this boils down to the wave equation (1.1) or (1.2), linearize by perturbation analysis. Introduce small perturbations around the state where $u = 0$ and $p = P_0$, by $u(x,t) = \epsilon\tilde{u}(x,t)$, $p(x,t) = P_0 + \epsilon\tilde{p}(x,t)$, and $\rho(x,t) = R(x) + \epsilon\tilde{\rho}(x,t)$ to get

$$
\begin{aligned}
&\epsilon\tilde{p}_t + \epsilon^2\tilde{u}\tilde{p}_x + c^2\left(R + \epsilon\tilde{\rho}\right)\epsilon\tilde{u}_x = 0\,,\\
&\left(R + \epsilon\tilde{\rho}\right)\left(\epsilon\tilde{u}_t + \epsilon^2\tilde{u}\tilde{u}_x\right) + \epsilon\tilde{p}_x = 0\,.
\end{aligned}
$$

Now neglect the very small terms proportional to ϵ^2 and omit the tilde signs, to get a system of equations,

$$\begin{aligned} p_t + c^2 R u_x &= 0\,, \\ u_t + R^{-1} p_x &= 0\,, \end{aligned}$$

or the acoustic wave equation of second order,

$$\frac{1}{c^2} p_{tt} = -R u_{xt} = -R u_{tx} = R\left(R^{-1} p_x\right)_x\,.$$

We now turn to a second application, plane electromagnetic wave propagation, with the electric field $\boldsymbol{E} = (0, E(x,t), 0)^T$ and the magnetic field $\boldsymbol{H} = (0, 0, H(x,t))^T$. For this one-dimensional problem, the Maxwell equations are simply

$$\begin{aligned} \frac{\partial H}{\partial t} &= -\frac{1}{\mu}\frac{\partial E}{\partial x}\,, \\ \frac{\partial E}{\partial t} &= -\frac{1}{\varepsilon}\frac{\partial H}{\partial x}\,, \end{aligned}$$

where μ is the magnetic permeability and ε is the electric conductivity. Identify $c^2 = (\mu\varepsilon)^{-1}$ and perform the derivations above. Hence we have the two decoupled wave equations

$$\begin{aligned} \frac{1}{c^2} H_{tt} &= \varepsilon\left(\frac{1}{\varepsilon} H_x\right)_x\,, \\ \frac{1}{c^2} E_{tt} &= \mu\left(\frac{1}{\mu} E_x\right)_x \end{aligned}$$

for the magnetic field and the electric field.

The application we primarily have in mind when developing the numerical methods is acoustic waves, where the computational domain is much larger than the wavelengths of the problems. For this we have, in accordance with the example above, the wave equation in one dimension in the form of (1.1),

$$\frac{1}{c^2} p_{tt} = \rho\left(\frac{1}{\rho} p_x\right)_x\,, \tag{1.3}$$

or the form of (1.2),

$$\begin{aligned} p_t &= -c^2 \rho\, u_x\,, \\ u_t &= -1/\rho\, p_x\,, \end{aligned} \tag{1.4}$$

now with ρ denoting the density. The propagation originates either from forcing functions F and G as above, or from initial and/or boundary conditions specifying inflow or outflow.

2 The Helmholtz equation

Now consider the case when (1.1), with $a(\boldsymbol{x}) > 0$ for all $\boldsymbol{x}$, has a time-periodic solution, so that ϕ and $\tilde{F}$ can be written as Fourier series

$$\phi(\boldsymbol{x},t) = \sum_{\omega} u_\omega(\boldsymbol{x}) e^{i\omega t}\,,$$
$$\tilde{F}(\boldsymbol{x},t) = \sum_{\omega} F_\omega(\boldsymbol{x}) e^{i\omega t}\,.$$

The problem of solving the wave equation is now reduced to the problem of solving the Helmholtz equation

$$a(\boldsymbol{x})\,\nabla\cdot\big(b(\boldsymbol{x})\,\nabla u_\omega(\boldsymbol{x})\big) + \omega^2 u_\omega(\boldsymbol{x}) = -F_\omega(\boldsymbol{x})\,. \tag{1.5}$$

The Helmholtz problem, corresponding to (1.3) and (1.4), is

$$\rho\left(\frac{1}{\rho}u'_\omega(x)\right)' + \kappa^2 u_\omega(x) = 0\,,$$

with $\kappa = \omega/c(x)$, or in homogenous media

$$u''(x) + \kappa^2 u(x) = 0\,, \tag{1.6}$$

together with boundary conditions.

3 Numerical solution methods

For both the time-dependent wave equation and the time-independent Helmholtz equation, we want to limit the number of values we store during the computations, and if we need to solve systems of linear equations, the coefficient matrices should have a narrow bandwidth. In other words, we are looking for methods with a compact "computational stencil".

In the following parts, we will study methods for, in order, (1.1), (1.2), and (1.5) following two main principles. The first idea is to repeatedly use the equation to cancel error terms if possible, originally used by Numerov in the 20's for ODEs, see the original papers [20, 21] and the classical textbook [5] as well as the newer works [1,4,22,23,26]. The second idea is due to Fox and much used by Pereyra for many years, see e.g. [9, 24]. The approach here is to use a lower order, more cheaply computed, solution for correction of error terms. Examples of recent work include [11–13, 15, 16].

When computing solutions to the wave equation, there is often a need to impose absorbing boundary conditions of Engquist-Majda type [6] to limit the area of computation. These well-posed boundary conditions minimize the artificial reflections from the boundary. For (1.1) with $a = b = 1$ in $\boldsymbol{x} \geqslant 0, t \geqslant 0$, the first absorbing boundary condition of this family at the line $x = L$ is

$$\left.\frac{\partial \phi}{\partial t} + \frac{\partial \phi}{\partial x}\right|_{x=L} = 0.$$

In one dimension, this outflow condition at $x = L$ is exact, giving $\phi = \phi(x - t)$. Unfortunately, we are only aware of stable discretizations of second order accuracy, but not of higher order! If we instead work with the Helmholtz equation (1.6), this is not a problem. To suppress all reflections at $x = L$ and allow only solutions like $u = \sigma e^{i\omega x}$, giving $\phi = \sigma e^{i\omega(x-t)}$, we use

$$u'(L) - i\kappa u(L) = 0\,.$$

This can easily be approximated to any order, using the formulas in the next chapter.

In Chapter 2, we compare higher order methods for the one-dimensional Helmholtz equation, and include a comment on the multi-dimensional case. The comparison is done based on sharp error predictions, confirmed by numerical experiments. Chapter 3 treats the one-dimensional wave equation in second order form as well as written as a system of first order equations, where the variables in the second case reside on staggered grids. Stability limits and norm-conserving properties are derived, and numerical experiments are presented that are in accordance with the expected accuracy order.

3.1 Notation

Throughout the text, we use the following notation when $h = x_j - x_{j-1}$, $k = t_n - t_{n-1}$, and $u_j^n = u(x_j, t_n)$:

$$\begin{aligned}
D_+ u_j &= \frac{u_{j+1} - u_j}{h}\,, \qquad & D_- u_j &= \frac{u_j - u_{j-1}}{h}\,,\\
D_0 u_j &= \frac{u_{j+1} - u_{j-1}}{2h}\,, & &\\
D_{1/2} u_j &= \frac{u_{j+1} + u_j}{2}\,, & D_{-1/2} u_j &= \frac{u_j + u_{j-1}}{2}\,.
\end{aligned}$$

These are the standard finite difference approximations of space derivatives, and $u_{j+1/2}$ computed as an average from the surrounding grid points. For time derivatives, we use the expressions

$$D_+^t u^n = \frac{u^{n+1} - u^n}{k}\,, \qquad D_-^t u^n = \frac{u^n - u^{n-1}}{k}\,.$$

Chapter 2

Higher order finite difference methods for the Helmholtz equation

1 Introduction

Today, the motion of waves is of fundamental importance in areas such as acoustics and electromagnetics. The propagation is described by the wave equation (1.1). For problems with solutions periodic in time, the solution of the wave equation is reduced to the solution of the Helmholtz equation (1.5).

In the applications above, the wave number κ may be very high, and such cases give rise to demanding problems, since the number of grid points must be large enough to resolve the oscillations. A low order standard solution method puts a restrictive demand on the resolution, and leads to a very large system of linear equations, so a higher order method is preferred. Here, the focus is on finite difference methods for discretizations on equidistant grids, that results in highly structured algebraic problems. For wave propagation problems on first order form, higher order methods have been examined in several papers, starting with the pioneering work by Kreiss and Oliger in [18], followed up by an analysis of fully discrete approximations a few years later in [25] written by Swartz and Wendroff. Since it is now known that higher order methods are indeed a more efficient way to solve first order wave problems, it is interesting to study higher order methods also for the Helmholtz equation.

Consider the one-dimensional case with constant coefficients (1.6).

$$u''(x) + \kappa^2 u(x) = 0, \qquad 0 < x < 1, \tag{2.1a}$$

subject to mixed boundary conditions

$$
\begin{aligned}
u'(0) + i\kappa u(0) &= 2i\kappa, \\
u'(1) - i\kappa u(1) &= 0.
\end{aligned}
\tag{2.1b}
$$

The boundary conditions model a source on the left hand boundary and ensure that problem (2.1) has the solution

$$u(x) = e^{i\kappa x},$$

which is the Fourier coefficient of a wave propagating from left to right for a corresponding wave equation problem.

In this chapter, the model problem (2.1) is used to discuss higher order finite difference methods for the Helmholtz equation for large κ. In Section 2, three different higher order methods are presented and the errors for the computed solutions are analyzed. In Sections 3 and 4, the methods are evaluated and ranked based on the derived expressions, and numerical experiments verify the results. Finally, Section 5 contains a discussion on what the results indicate for the case (1.5) with variable coefficients.

2 Three finite difference methods

Define a uniform grid by $x_j = (j - \frac{1}{2})h$, $h = 1/n$, so that the grid points are centered around the endpoints of the interval. A second order accurate solution $u^{<2>}$ to (2.1), discretized on this grid, is found by the centered scheme

$$\left[h^2 D_+ D_- + \alpha^2\right] u_j^{<2>} = 0, \quad j = 1, \ldots, n, \tag{2.2a}$$

$$
\begin{aligned}
\left[hD_+ + i\alpha D_{1/2}\right] u_0^{<2>} &= 2i\alpha, \\
\left[hD_- - i\alpha D_{-1/2}\right] u_{n+1}^{<2>} &= 0.
\end{aligned}
\tag{2.2b}
$$

The solution to this linear difference equation is found by the ansatz

$$u_j^{<2>} = \sigma_1 z_1^{(j-\frac{1}{2})} + \sigma_2 z_2^{(j-\frac{1}{2})}.$$

The characteristic equation of (2.2a),

$$(z-1)^2 + \alpha^2 z = 0,$$

has two roots z_1 and z_2 with

$$z_1 = \overline{z_2} = e^{i\beta},$$

and

$$\beta = \arccos\left(1 - \alpha^2/2\right) = \alpha + \frac{1}{24}\alpha^3 + \mathcal{O}(\alpha^5) = \kappa h + \frac{1}{24}\kappa^3 h^3 + \mathcal{O}(h^5),$$

for a sufficiently small h. The boundary conditions (2.2b) give

$$\sigma_1 = 1 + \frac{1}{16}\kappa^2 h^2 + \mathcal{O}(h^4),$$
$$\sigma_2 = \frac{1}{16}\zeta\kappa^2 h^2 + \mathcal{O}(h^4), \text{ with } \zeta = e^{2i\kappa}, \ |\zeta| = 1.$$

The accuracy of the scheme is of order two, measured in ℓ_2-norm, but in order to resolve the wave solution, the phase error, depending on κ, must be controlled. For this second order standard scheme, the analysis is performed in a similar way by Otto and Larsson in [23].

When compared with the analytical solution of (2.1),

$$u(x_j) = e^{i\kappa x_j},$$

the shift in the argument is found to be linearly dependent on x:

$$u_j^{<2>} = \sigma_1 u(x_j) e^{i\left(\frac{1}{24}\kappa^3 h^2 + \mathcal{O}(h^4)\right)x_j} + \sigma_2 e^{-i\left(\kappa + \frac{1}{24}\kappa^3 h^2 + \mathcal{O}(h^4)\right)x_j}.$$

The phase error is $\mathcal{O}(\kappa^3 h^2)$, while the amplitude error is $\mathcal{O}(\kappa^2 h^2)$. Hence the largest value of the leading term of the phase shift for the right-going wave is used as a resolution tolerance. For a prescribed tolerance ε, use

$$\frac{1}{24}\kappa^3 h^2 = \varepsilon,$$

or

$$n^{<2>} = (h^{<2>})^{-1} = \left(\frac{\kappa^3}{24\varepsilon}\right)^{1/2}.$$

For this grid spacing the amplitudes of the right- and left-going waves are

$$\sigma_1 = 1 + \frac{3}{2}\kappa^{-1}\varepsilon + \mathcal{O}(\kappa^{-2}),$$
$$\sigma_2 = \frac{3}{2}\zeta\kappa^{-1}\varepsilon + \mathcal{O}(\kappa^{-2}).$$

This shows that for the large values of κ that are of interest, the error in the solution is dominated by the phase shift,

$$|u_j^{<2>} - u(x_j)| \approx \frac{1}{24}\kappa^3 h^2 x_j. \tag{2.3}$$

The result of computations with a large error due to an insufficient number of grid points is illustrated in Figure 2.1. Since the real and the imaginary parts are affected in the same way, Figure 2.2 presents only the real parts of the differences between the computed and the true solutions for a small and a large wave number κ.

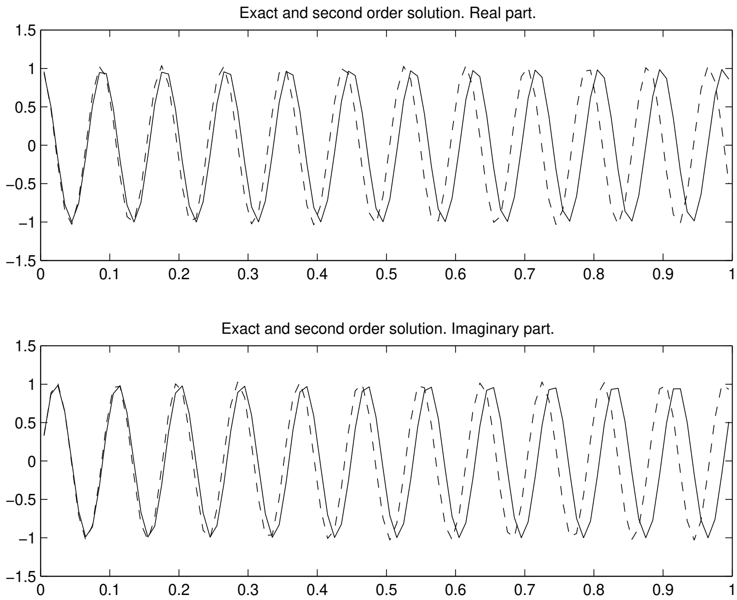

Figure 2.1: The dominating part of the error is the phase shift. Here, $\kappa = 70$ and the number of grid points have been set to 100 to visualize this.

2.1 Wide high order scheme

The investigation of higher order methods is started with wide schemes where higher order derivatives in the truncation error are gradually eliminated by centered approximations. The numerical solution of order p at $x = x_j$ obtained by these schemes will be denoted by $u_j^{<p>}$. Since

$$\begin{aligned} D_+D_-u(x_j) &= h^{-2}\left(u(x_j+h) - 2u(x_j) + u(x_j-h)\right) = \\ &= u''(x_j) + \frac{1}{12}h^2u''''(x_j) + \mathcal{O}(h^4), \end{aligned}$$

a fourth order scheme for the inner points is obtained by

$$\left[\left(I - \frac{1}{12}h^2D_+D_-\right)h^2D_+D_- + \alpha^2\right]u_j^{<4>} = 0, \quad j = 1, \ldots, n, \tag{2.4a}$$

resulting in a pentadiagonal system of linear equations to be solved.

For the boundaries, conditions (2.1b) have to be applied at points centered

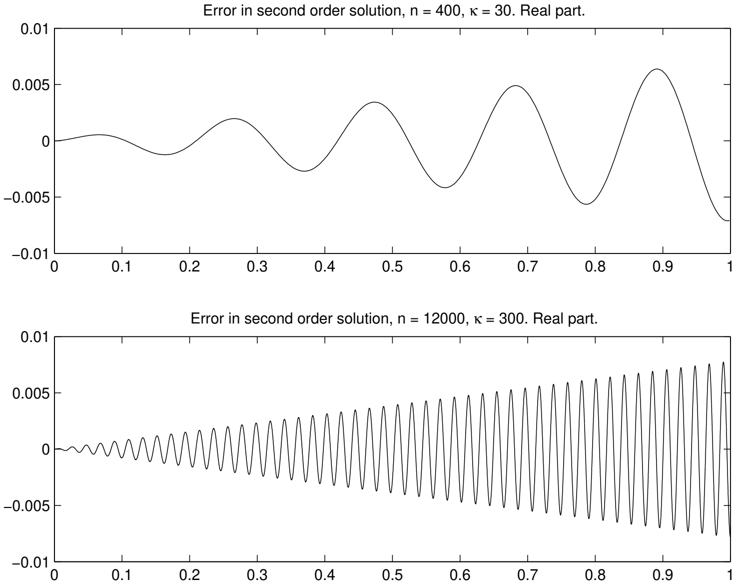

Figure 2.2: The numerical test confirms (2.3), the magnitude of the error for the second order scheme is proportional to x.

around $x = 0$ and $x = 1$:

$$D_+u(x_0) = h^{-1}\left(u(\frac{h}{2}) - u(-\frac{h}{2})\right) = u'(0) + \frac{1}{24}h^2u'''(0) + \mathcal{O}(h^4),$$
$$D_{1/2}u(x_0) = \frac{1}{2}\left(u(\frac{h}{2}) + u(-\frac{h}{2})\right) = u(0) + \frac{1}{8}h^2u'''(0) + \mathcal{O}(h^4),$$

and analogous expressions for $D_-u(x_{n+1})$ and $D_{-1/2}u(x_{n+1})$ give

$$\text{(2.4b)}\quad \begin{aligned} &\left[\left(I - \frac{1}{24}h^2D_+D_-\right)hD_+ + i\alpha\left(I - \frac{1}{8}h^2D_+D_-\right)D_{1/2}\right]u_0^{<4>} = 2i\alpha, \\ &\left[\left(I - \frac{1}{24}h^2D_+D_-\right)hD_- - i\alpha\left(I - \frac{1}{8}h^2D_+D_-\right)D_{-1/2}\right]u_{n+1}^{<4>} = 0. \end{aligned}$$

In the application of the new stencils, extra ghost points outside the interval are needed. To keep the accuracy of the method, their values are set by polynomial extrapolation:

$$\text{(2.4c)}\qquad (hD_+)^6\, u_{-1}^{<4>} = (hD_-)^6\, u_{n+2}^{<4>} = 0.$$

The solution to (2.4a) is

$$u_j^{<4>} = \sum_{k=1}^{4} \sigma_k z_k^{(j-\frac{1}{2})},$$

where $\{z_k\}_{k=1}^4$ are the roots of the characteristic equation

$$\left(z - \frac{1}{12}(z-1)^2\right)(z-1)^2 + \alpha^2 z^2 =$$
$$= -\frac{1}{12}\left[\left(z^2 - 2\left(4 - \sqrt{9+3\alpha^2}\right)z + 1\right)\left(z^2 - 2\left(4 + \sqrt{9+3\alpha^2}\right)z + 1\right)\right] = 0.$$

The pair of roots z_1 and z_2 are complex conjugate and lies on the unit circle, representing an approximation to the true solution and the reflection of that, with

$$z_1 = e^{i\beta}, \text{ where } \beta = \arccos\left(4 - \sqrt{9+3\alpha^2}\right) = \alpha + \frac{1}{180}\alpha^5 - \frac{1}{2016}\alpha^7 + \mathcal{O}(\alpha^9).$$

There are also two real valued parasitic solutions z_3 and z_4. From the boundary conditions (2.4b) and (2.4c), it is seen that

$$\sigma_1 = 1 + \mathcal{O}(h^4),$$
$$\sigma_2 = \mathcal{O}(h^4), \quad \sigma_3 = \mathcal{O}(h^4), \quad \sigma_4 = \mathcal{O}(h^4),$$

and

$$u_j^{<4>} \approx u(x_j)e^{i\left(\frac{1}{180}\kappa^5 h^4 + \mathcal{O}(h^6)\right)x_j} + \mathcal{O}(\kappa^4 h^4),$$

so the error

$$|u_j^{<4>} - u(x_j)| \approx \frac{1}{180}\kappa^5 h^4 x_j. \tag{2.5}$$

is again dominated by the phase shift, verified in Figure 2.3. By using the same arguments as for the second order method, the number of unknowns is chosen as

$$n_u^{<4>} = \left(\frac{\kappa^5}{180\varepsilon}\right)^{1/4}.$$

Now, note that since

$$\left(I - \frac{1}{12}h^2 D_+ D_-\right) D_+ D_- u(x_j) = u''(x_j) - \frac{1}{90}h^4 u^{(6)}(x_j) + \mathcal{O}(h^6),$$

and with similar expansions for the boundary expressions, a sixth order scheme resulting in a hepta-diagonal system can be constructed:

$$\left[\left(I - \frac{1}{12}h^2 D_+ D_- + \frac{1}{90}h^4 (D_+ D_-)^2\right) h^2 D_+ D_- + \alpha^2\right] u_j^{<6>} = 0, \tag{2.6a}$$
$$j = 1, \ldots, n,$$

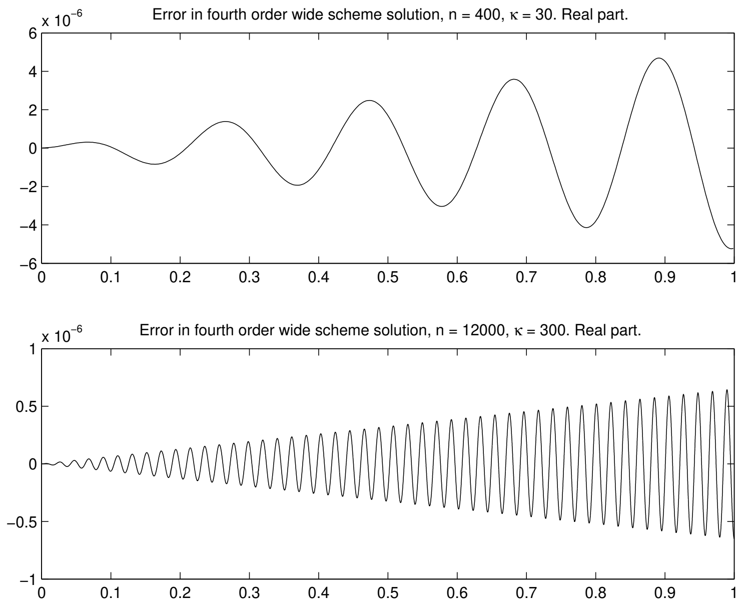

Figure 2.3: The error (2.5) of the solution computed with a fourth order wide scheme.

$$\begin{aligned}
&\Big[\Big(I - \frac{1}{24}h^2 D_+D_- + \frac{3}{640}h^4 (D_+D_-)^2\Big)\, hD_+ + \\
&\qquad + \Big(I - \frac{1}{8}h^2 D_+D_- + \frac{3}{128}h^4 (D_+D_-)^2\Big)\, i\alpha D_{1/2}\Big] u_0^{<6>} = 2i\alpha, \\
&\Big[\Big(I - \frac{1}{24}h^2 D_+D_- + \frac{3}{640}h^4 (D_+D_-)^2\Big)\, hD_- - \\
&\qquad + \Big(I - \frac{1}{8}h^2 D_+D_- + \frac{3}{128}h^4 (D_+D_-)^2\Big)\, i\alpha D_{-1/2}\Big] u_{n+1}^{<6>} = 0.
\end{aligned} \tag{2.6b}$$

Here, two additional grid points on each side are needed, and are defined by high order extrapolation:

$$\begin{aligned}
(hD_+)^8\, u_{-1}^{<6>} &= (hD_-)^8\, u_{n+2}^{<6>} = 0, \\
(hD_+)^8\, u_{-2}^{<6>} &= (hD_-)^8\, u_{n+3}^{<6>} = 0.
\end{aligned} \tag{2.6c}$$

In the same way as above, a Taylor series expansion in h of the solution to this difference equation yields

$$\varepsilon^{<6>} = \max |u_j^{<6>} - u(x_j)| \approx \max \frac{1}{1120} h^6 \kappa^7 x_j = \frac{1}{1120} h^6 \kappa^7, \tag{2.7}$$

giving

$$n_u^{<6>} = \left(\frac{\kappa^7}{1120\varepsilon}\right)^{1/6}.$$

This prediction of the error's behavior is confirmed by experiments shown in Figure 2.4. Here, the reflected solution, going from right to left, is visible, but it is much smaller than the error in the right-going solution.

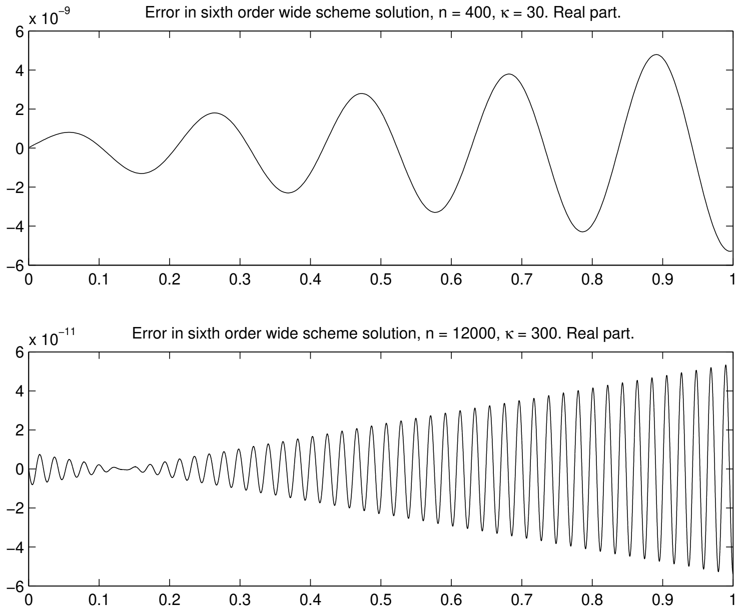

Figure 2.4: The error (2.7) of the solution computed with a sixth order wide scheme.

The weights for the stencils constructed according to this simple principle of subtraction of higher derivatives are straightforward to find. This can be done manually or e.g. by the technique described in [8]. But for increased accuracy, the stencils get wider and wider, and in addition to the inflation in complexity to solve the resulting systems of equations, this may also cause problems for decomposition techniques for parallel implementations. Therefore, in the remainder of this chapter, alternative schemes with more compact stencils will be discussed.

2.2 The Numerov scheme

In this section, higher order methods of Numerov type (originally in [20,21], but more widely known from Collatz [5]) for the Helmholtz equation are designed. By repeated usage of equation (2.1a), compact stencils giving narrow-banded systems of linear equations are found. Below, the notation $v_j^{<p>}$ is used for the solution to distinguish it from $u_j^{<p>}$ in the previous section.

Since

$$\begin{aligned} D_+D_-u(x_j) &= h^{-2}\left(u(x_j+h) - 2u(x_j) + u(x_j-h)\right) = \\ &= u''(x_j) + \frac{1}{12}h^2u''''(x_j) + \mathcal{O}(h^4), \end{aligned}$$

and, from (2.1a),

$$u''''(x_j) = -\kappa^2 u''(x_j)$$

for all inner points x_j, it is seen that

$$\left[\left(I + \frac{1}{12}\alpha^2\right) D_+D_-\right] u(x_j) = u''(x_j) + \mathcal{O}(h^4).$$

The same kind of manipulations for the boundary conditions give the fourth order scheme

$$\left[\left(I + \frac{1}{12}\alpha^2\right) h^2 D_+D_- + \alpha^2\right] v_j^{<4>} = 0, \quad j = 1, \ldots, n, \tag{2.8a}$$

$$\begin{aligned} \left[\left(I + \frac{1}{24}\alpha^2\right) hD_+ + i\alpha\left(I + \frac{1}{8}\alpha^2\right) D_{1/2}\right] v_0^{<4>} &= 2i\alpha, \\ \left[\left(I + \frac{1}{24}\alpha^2\right) hD_- - i\alpha\left(I + \frac{1}{8}\alpha^2\right) D_{-1/2}\right] v_{n+1}^{<4>} &= 0. \end{aligned} \tag{2.8b}$$

The roots of the characteristic equation of (2.8a) are

$$e^{\pm i\beta} \text{ with } \beta = \arccos\left(1 - \frac{\alpha^2/2}{1+\alpha^2/12}\right) = \kappa h + \frac{1}{480}\kappa^5 h^5 + \mathcal{O}(h^7).$$

Substituting this into the boundary conditions (2.8b) gives

$$\sigma_1 = 1 + \mathcal{O}(h^4), \quad \sigma_2 = \mathcal{O}(h^4).$$

The grid for resolution with maximum error ε is again determined by the phase error and proportional to x, giving

$$\varepsilon^{<4>} = \frac{1}{480}\kappa^5 h^4, \tag{2.9}$$

and

$$n_v^{<4>} = \left(\frac{\kappa^5}{480\varepsilon}\right)^{1/4}.$$

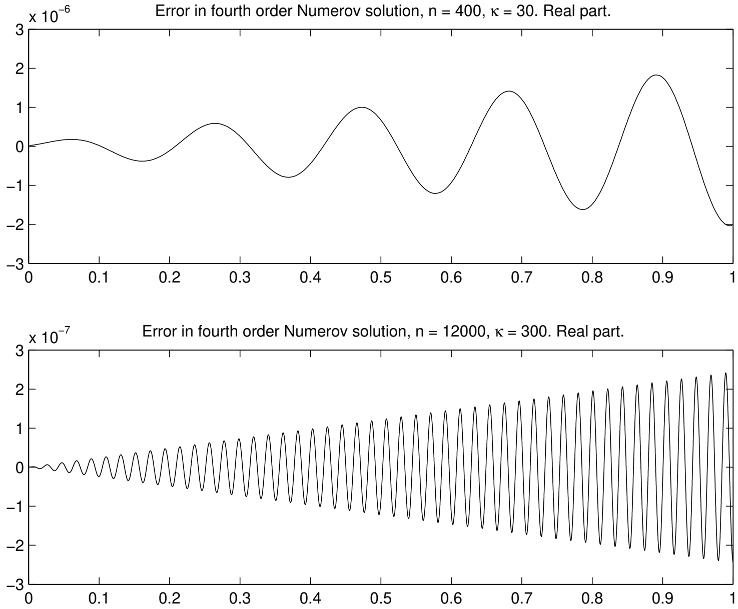

Figure 2.5: The fourth order accuracy Numerov method has a smaller error (2.9) than the fourth order wide scheme.

Note that not only are extra points and a wide-banded system of equation avoided, but for given κ and h, the constant in the leading error term is reduced with a factor $8/3$ compared to the wide centered fourth order scheme, see Figure 2.5!

Now observe that

$$\left[\left(I + \frac{1}{12}\alpha^2\right) D_+D_-\right] u(x_j) = u''(x_j) - \frac{1}{240}h^4 u^{(6)}(x_j) + \mathcal{O}(h^6),$$

and use the Helmholtz equation (2.1) again, to get the sixth order compact scheme

$$\left[\left(I + \frac{1}{12}\alpha^2 + \frac{1}{240}\alpha^4\right) h^2 D_+D_- + \alpha^2\right] v_j^{<6>} = 0, \quad j = 1, \ldots, n, \tag{2.10a}$$

$$
\begin{aligned}
&\left[\left(I+\frac{1}{24}\alpha^2+\frac{7}{5760}\alpha^4\right)hD_+ + \right.\\
&\qquad\left. + i\alpha\left(I+\frac{1}{8}\alpha^2+\frac{5}{384}\alpha^4\right)D_{1/2}\right]v_0^{<6>} = 2i\alpha,\\
&\left[\left(I+\frac{1}{24}\alpha^2+\frac{7}{5760}\alpha^4\right)hD_- - \right.\\
&\qquad\left. - i\alpha\left(I+\frac{1}{8}\alpha^2+\frac{5}{384}\alpha^4\right)D_{-1/2}\right]v_{n+1}^{<6>} = 0
\end{aligned}
\tag{2.10b}
$$

This scheme has the small phase error (Figure 2.6)

$$
\frac{1}{12096}\kappa^7 h^6 x_j, \tag{2.11}
$$

so in order to resolve the wave,

$$
n_v^{<6>} = \left(\frac{\kappa^7}{12096\varepsilon}\right)^{1/6}
$$

grid points are enough.

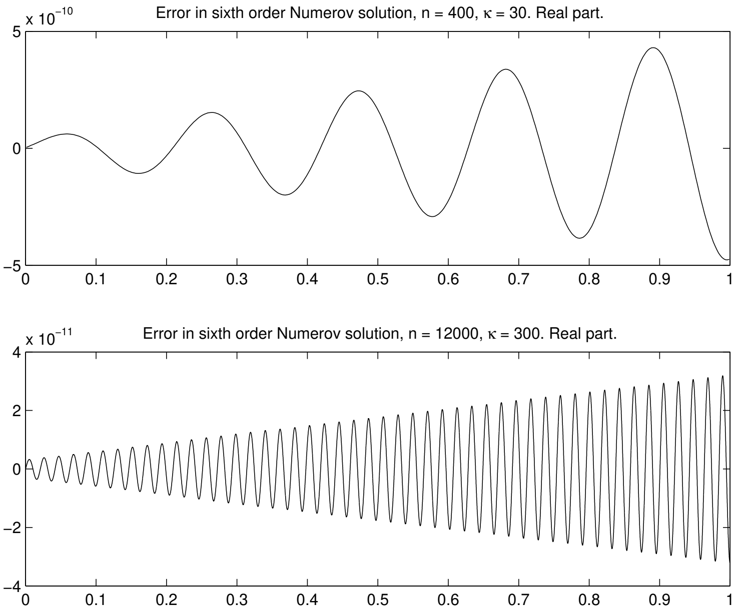

Figure 2.6: The error (2.11) of the solution computed with a compact Numerov scheme of accuracy order six.

The Numerov scheme of order $2p$ for problem (2.1) can be found by the following algorithm

$$
\begin{aligned}
& a_0 = b_0 = c_0 = -1, \\
& k = 1, 2, \ldots, p-1: \\
& \quad \alpha_k = 2 \cdot (-1)^k \cdot \frac{1}{(2k+2)!}, \quad \beta_k = (-1)^k \cdot \frac{1}{4^k} \cdot \frac{1}{(2k+1)!}, \quad \gamma_k = \frac{1}{2}\beta_k, \\
& \ell = 1, 2, \ldots, p-1: \\
& \quad a_\ell = -\sum_{k=0}^{\ell-1} a_k \alpha_{\ell-k}, \quad b_\ell = -\sum_{k=0}^{\ell-1} b_k \beta_{\ell-k}, \quad c_\ell = -\sum_{k=0}^{\ell-1} c_k \gamma_{\ell-k}, \\
& u''(x_j) = \left[-\sum_{\ell=0}^{p-1} a_\ell \left(h^2\kappa^2\right)^\ell \right] D_+ D_- v_j + \mathcal{O}(h^{2p}), \\
& u'(x_j + h/2) = \left[-\sum_{\ell=0}^{p-1} b_\ell \left(h^2\kappa^2\right)^\ell \right] D_+ v_j + \mathcal{O}(h^{2p}), \\
& u(x_j + h/2) = \left[-\sum_{\ell=0}^{p-1} c_\ell \left(h^2\kappa^2\right)^\ell \right] D_{1/2} v_0 + \mathcal{O}(h^{2p}).
\end{aligned}
$$

2.3 Deferred correction

The method of deferred correction, originally introduced by Fox [9] and further developed by Pereyra in a series of papers, starting with [24], is another and more general way to maintain a narrow bandwidth of a system arising from a discretization. The idea is to use lower order approximations of high derivatives to eliminate terms in the truncation error. These approximations are not, as in Section 2.1, applied to the unknowns, but to values from a previous computational step. This gives a procedure where one solves a sequence of systems, all with the same coefficient matrix, but with different right hand sides.

Assume that a second order solution $w_j^{<2>}$ has been computed with the standard scheme (2.2). Then use this solution to construct the fourth order scheme

$$
\left[h^2 D_+ D_- + \alpha^2\right] w_j^{<4>} = \frac{1}{12} h^4 (D_+ D_-)^2 w_j^{<2>}, \quad j = 1, \ldots, n, \tag{2.12a}
$$

$$
\begin{aligned}
& \left[hD_+ + i\alpha D_{1/2}\right] w_0^{<4>} = 2i\alpha + \\
& \qquad + \left[\frac{1}{24} h^3 D_+^2 D_- + i\alpha \frac{1}{8} h^2 D_+ D_- D_{1/2}\right] w_0^{<2>}, \\
& \left[hD_- - i\alpha D_{-1/2}\right] w_{n+1}^{<4>} = \\
& \qquad = \left[\frac{1}{24} h^3 D_+ D_-^2 - i\alpha \frac{1}{8} h^2 D_+ D_- D_{-1/2}\right] w_{n+1}^{<2>}.
\end{aligned} \tag{2.12b}
$$

The scheme requires $w^{<2>}$ (but not the unknown $w^{<4>}$) to be defined at two additional points outside the interval. This is done as in [11] by extrapolation with a polynomial of order six to maintain the accuracy of the scheme:

$$(hD_+)^6\, w_{-1}^{<2>} = (hD_-)^6\, w_{n+2}^{<2>} = 0.$$

When solving (2.12a) for $w_j^{<4>}$, the right hand side has factors that are roots of the characteristic polynomial for the left hand side. A particular solution is

$$w_{j,p}^{<4>} = -\left(\frac{1}{24}i\alpha^3 + \frac{1}{192}i\alpha^5 + \mathcal{O}(\alpha^7)\right)\cdot j\cdot\left(\sigma_1 e^{i\beta(j-\frac{1}{2})} - \sigma_2 e^{-i\beta(j-\frac{1}{2})}\right),$$

with σ_1, σ_2 and β from the solution to (2.2). After insertion of the solution

$$w_j^{<4>} = \sigma_3 e^{i\beta(j-\frac{1}{2})} + \sigma_4 e^{-i\beta(j-\frac{1}{2})} + w_{j,p}^{<4>}$$

into (2.12b), a Taylor series expansion shows that

$$w_j^{<4>} \approx \left(1 - \frac{1}{24}i\kappa^3 h^2 x_j\right) e^{i(\kappa+\frac{1}{24}\kappa^3 h^2)x_j}.$$

The error in the computed solution will increase going from the left boundary to the right, not only with the growing phase shift, but also as a noticeable increase in amplitude. Examples of this are shown in Figures 2.7 and 2.8.

Since the phase error at the right boundary is $\frac{1}{24}\kappa^3 h^2$, the same number of grid points as for the standard second order scheme is enough to resolve this. Unfortunately, because of the amplitude error, the total error in the solution is proportional not to $\kappa^5 h^4$, but to $\kappa^6 h^4$:

$$|w_j^{<4>} - u(x_j)| \approx \frac{1}{1152}\kappa^6 h^4 x_j^2. \tag{2.13}$$

Therefore, it is necessary to use

$$n_w^{<4>} = \left(\frac{\kappa^6}{1152\varepsilon}\right)^{1/4}$$

grid points, which is larger than the corresponding number of grid points for the wide stencil scheme and the Numerov scheme.

To derive a sixth order deferred correction scheme for the inner points, $w_j^{<4>}$ is computed and extended to two extra points on each side of the interval by interpolation:

$$(hD_+)^8\, w_{-1}^{<4>} = (hD_-)^8\, w_{n+2}^{<4>} = 0,$$
$$(hD_+)^8\, w_{-2}^{<4>} = (hD_-)^8\, w_{n+3}^{<4>} = 0.$$

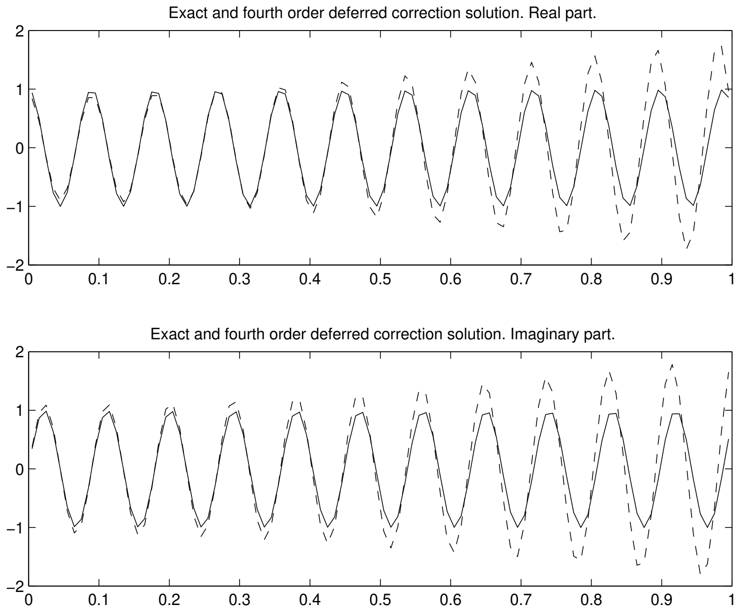

Figure 2.7: For the deferred correction method, both a phase shift and an amplitude growth is present.

The sixth order scheme is then

$$\left[h^2 D_+ D_- + \alpha^2\right] w_j^{<6>} = \left[\frac{1}{12} h^4 (D_+ D_-)^2 - \frac{1}{90} h^6 (D_+ D_-)^3\right] w_j^{<4>}, \quad j = 1, \ldots, n, \tag{2.14a}$$

$$\begin{aligned}
\left[hD_+ + i\alpha D_{1/2}\right] w_0^{<6>} &= 2i\alpha + \\
&+ \left[\left(\frac{1}{24} h^2 D_+ D_- - \frac{3}{640} h^4 (D_+ D_-)^2\right) hD_+ + \right. \\
&\left. + i\alpha \left(\frac{1}{8} h^2 D_+ D_- - \frac{3}{128} h^4 (D_+ D_-)^2\right) D_{1/2}\right] w_0^{<4>}, \\
\left[hD_- - i\alpha D_{-1/2}\right] w_{n+1}^{<6>} &= \left[\left(\frac{1}{24} h^2 D_+ D_- - \frac{3}{640} h^4 (D_+ D_-)^2\right) hD_- - \right. \\
&\left. - i\alpha \left(\frac{1}{8} h^2 D_+ D_- - \frac{3}{128} h^4 (D_+ D_-)^2\right) D_{-1/2}\right] w_{n+1}^{<4>}.
\end{aligned} \tag{2.14b}$$

The solution to this (see Figures 2.9 and 2.10) is

$$w_j^{<6>} \approx \left(1 - \frac{1}{24} i\kappa^3 h^2 x_j - \frac{1}{1152} \kappa^6 h^4 x_j^2\right) e^{i(\kappa + \frac{1}{24}\kappa^3 h^2) x_j},$$

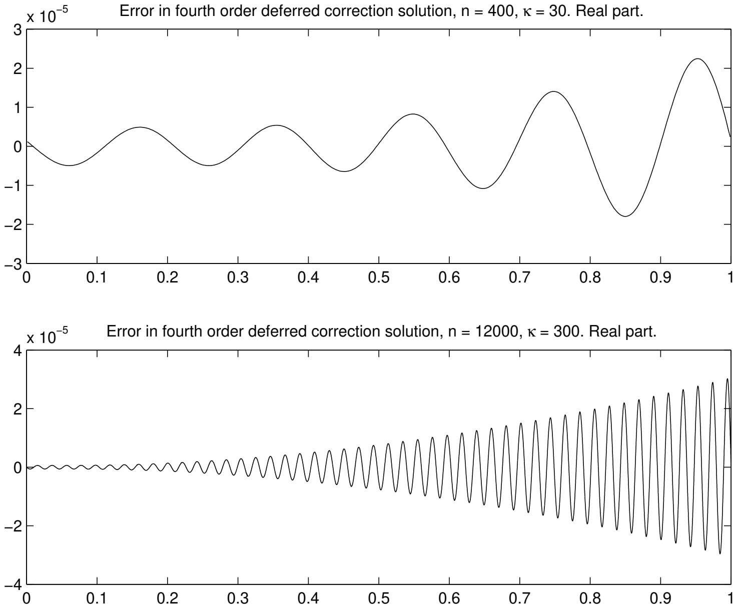

Figure 2.8: The magnitude of the error in the fourth order deferred correction method is proportional to x^2, as shown in (2.13).

with

$$|w_j^{<6>} - u(x_j)| \approx \frac{1}{82944}\kappa^9 h^6 x_j^3, \tag{2.15}$$

which is an error of order h^6 by construction, but proportional to x^3 and to the possibly very large κ^9. Hence,

$$n_w^{<6>} = \left(\frac{\kappa^9}{82944\varepsilon}\right)^{1/6}.$$

is the necessary number of grid points.

3 Work complexity comparisons

A fair comparison of the different methods can be done by prescribing the error tolerance ε, use just enough points in the grid to get this error, and find out how many arithmetic operations that have to be performed to find the solution. As the objective here is to rank the different schemes, the banded systems of equations are solved by direct methods. For real applications and multidimensional problems (see Section 5), iterative solvers should be considered.

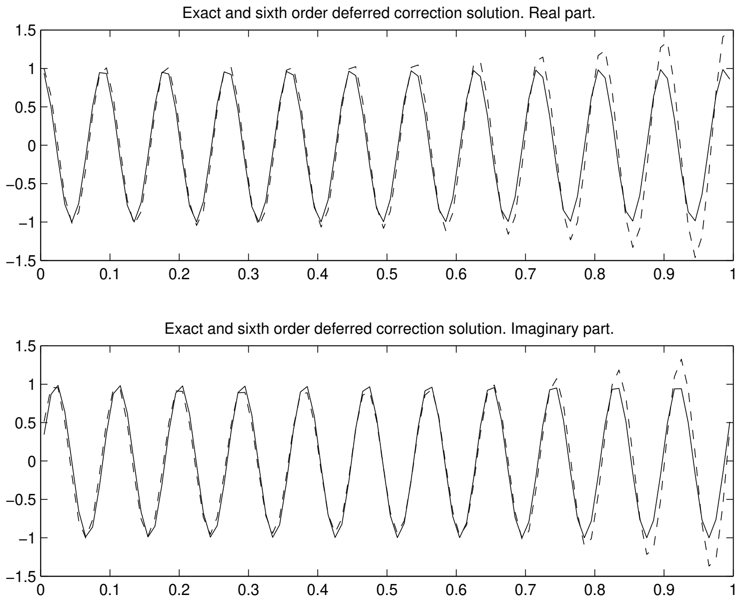

Figure 2.9: Computation showing phase and amplitude error for a sixth order deferred correction solution.

The second order method and all the Numerov schemes give tridiagonal systems of equations of order $n+2$ and zero right hand sides (except for one element). To solve these, approximately $8n$ arithmetic operations are needed. For penta- and hepta-diagonal systems of order n, the corresponding work is [10] $19n$ and $34n$ operations, respectively. With fourth order deferred correction, first solve the tridiagonal system for $u^{<2>}$, construct the right hand side in $7n$ operations, and finally solve the new tridiagonal system. In total, this is $23n$ operations. For sixth order deferred correction, this is further increased to $41n$ operations.

To study how much is gained by higher order methods, and to make a comparison between schemes, the work is normalized with respect to the second order method. Table 2.1 shows the predicted ratios for the work based on equal error ε for different κ. For every combination of these parameters in the table, a higher order scheme is predicted to be faster than a lower order one , and a Numerov scheme beats a wide scheme that in turn beats a deferred correction scheme.

4 Numerical results

In order to get an indication of how well the ratios in Table 2.1 agree with real computations, the solvers were implemented in MATLAB and the cpu-times

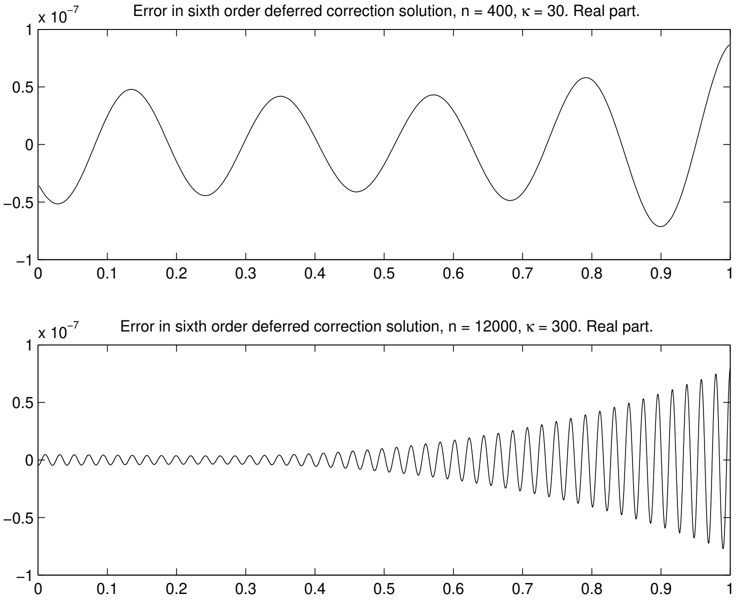

Figure 2.10: The magnitude of the error in the sixth order deferred correction method is proportional to x^3.

were measured. The results are shown in Table 2.2. For the standard second order scheme, the large number of unknowns leads to a more intricate memory handling, and the scaling factors become much larger than predicted. However, the numerical results for the higher order methods confirm the above ranking of the schemes. Clearly, higher order methods are undoubtedly more efficient, and for this MATLAB implementation, the coefficient matrix stemming from the second order method is to large for the computer memory.

5 What about real problems?

For the one-dimensional version of (1.5),

$$a(x)\big(b(x)u'(x)\big)' + \omega^2 u(x) = -F(x), \tag{2.16}$$

a wide scheme as in Section 2.1 is easily constructed for any even order of accuracy. However, the far-stretched stencil will be a problem close to the boundaries.

To construct a compact fourth order Numerov scheme for (2.16), one can follow the technique in a paper by Otto [22] to obtain a three-point wide scheme:

$$a_j D_+ \left(b_{j-\frac{1}{2}} D_- u_j\right) + \omega^2 u_j + h^2 \mathcal{A}(a_j, b_j, u_j) = -F_j + h^2 \mathcal{B}(a_j, b_j, F_j)$$

	$W^{<2>}/W^{<p>}$	κ	ε		
			10^{-4}	10^{-6}	10^{-8}
4th def. corr.	$\dfrac{8}{23}\dfrac{(1152\varepsilon)^{1/4}}{(24\varepsilon)^{1/2}}$	–	4	13	41
4th wide	$\dfrac{8}{19}\left(\dfrac{180\varepsilon}{\kappa^5}\right)^{1/4}\left(\dfrac{\kappa^3}{24\varepsilon}\right)^{1/2}$	10	6	18	56
		100	10	31	100
		1000	18	56	177
4th Numerov	$\left(\dfrac{480\varepsilon}{\kappa^5}\right)^{1/4}\left(\dfrac{\kappa^3}{24\varepsilon}\right)^{1/2}$	10	17	54	170
		100	30	96	302
		1000	54	170	537
6th def. corr	$\dfrac{8}{41}\dfrac{(82944\varepsilon)^{1/6}}{(24\varepsilon)^{1/2}}$	–	6	26	122
6th wide	$\dfrac{8}{34}\left(\dfrac{1120\varepsilon}{\kappa^7}\right)^{1/6}\left(\dfrac{\kappa^3}{24\varepsilon}\right)^{1/2}$	10	7	33	155
		100	15	72	333
		1000	33	155	718
6th Numerov	$\left(\dfrac{12096\varepsilon}{\kappa^7}\right)^{1/6}\left(\dfrac{\kappa^3}{24\varepsilon}\right)^{1/2}$	10	45	211	978
		100	98	454	2107
		1000	211	978	4539

Table 2.1: Work ratios for prescribed maximum error ε för different κ. A higher value indicates a more efficient method. All the higher order methods have a work ratio greater than one.

The exact formulas for, and the cost for calculating, $\mathcal{A}(a_j, b_j, u_j)$ and $\mathcal{B}(a_j, b_j, F_j)$ depend on whether $F'(x)$ and $F''(x)$ are available and how expensive the evaluations of $a(x)$ and $b(x)$ are. If this kind of discretization is allowed to be tailored for a specific problem, this is hard to outperform by a more general approach.

In the fourth order deferred correction algorithm for (2.16), no derivatives of F are needed, and second order approximations of the correction terms can all be obtained from the second order solution. However, as seen above, the formally fourth order error is proportional to κ^6, and therefore large for the values of κ that stimulate the use of a higher order methods.

For the multidimensional problem (1.5), it is possible that the sheer size of the problem will make a parallel implementation necessary, and that introduces extra, internal, boundaries in the domain. In two dimensions, a second order scheme consists of a five-point stencil, a fourth order wide scheme of a "thin" nine-point stencil and so on. The increased bandwidth can be handled by good iterative solvers, but any type of boundaries, outer or inner, need even more special attention, and for parallel implementations, the communication work increases rapidly.

The compact and efficient Numerov schemes in Section 2.2 are a little less

$\kappa = 100,\ \varepsilon = 10^{-6}$			
	n	time	$\max\lvert u^* - u\rvert$
4th def. corr.	5428	18.46	$1.0 \cdot 10^{-6}$
4th wide	2731	3.16	$1.0 \cdot 10^{-6}$
4th Numerov	2137	1.41	$1.0 \cdot 10^{-6}$
6th def. corr.	1515	2.16	$1.0 \cdot 10^{-6}$
6th wide	669	0.30	$1.1 \cdot 10^{-6}$
6th Numerov	450	0.07	$1.1 \cdot 10^{-6}$
$\kappa = 100,\ \varepsilon = 10^{-8}$			
	n	time	$\max\lvert u^* - u\rvert$
4th def. corr.	17165	195.98	$1.0 \cdot 10^{-8}$
4th wide	8634	31.79	$9.9 \cdot 10^{-9}$
4th Numerov	6757	14.41	$1.0 \cdot 10^{-8}$
6th def. corr.	3263	9.88	$1.0 \cdot 10^{-8}$
6th wide	1441	1.24	$1.0 \cdot 10^{-8}$
6th Numerov	969	0.29	$1.1 \cdot 10^{-8}$

Table 2.2: Cpu-times for the different methods. They correspond roughly to the predicted work in Table 2.1.

appealing for more than one dimension as they will contain approximations of mixed derivatives that enlarge the stencil. A fourth order Numerov method consists in two dimensions of a nine-point square stencil. In [22], the scheme is used to compute acoustic waves in a duct. For a general framework for fourth order compact schemes for the Helmholtz equation with constant coefficients and some other problems, see Boisvert's paper [1].

Even though deferred correction proved less suitable for the Helmholtz equation in the analysis, it can be the method of choice for two-dimensional (and three-dimensional) problems because of its simplicity! In the whole sequence of systems of equations to solve, the coefficient matrix will always be the same, originating from a five-point stencil in two dimensions and a seven-point stencil in three dimensions.

6 Conclusions

When solving the Helmholtz equation for increasing wavenumbers κ with low order methods, the grid soon becomes prohibitively fine. Here, sharp estimates of the errors for three different types of higher order finite difference methods are derived. A high order method based on wide centered stencils is trivial to construct for one or several dimensions, and is more efficient than the low order method despite the greater work complexity. Even better is to derive Numerov type methods by using the equation itself to maintain a narrow stencil. For these methods, the improvement obtained by increasing the order of accuracy is even greater for larger values of κ. The principle of deferred correction has a larger error on a given grid and cannot compete with the other two methods in efficiency for the one-dimensional Helmholtz equation portraited here, but has advantages in decomposition settings with internal boundaries in one or several dimensions.

Chapter 3

Higher order finite difference methods for the wave equation

1 Introduction

In this chapter, we will construct and compare explicit difference methods for solution of the wave equation (1.1) and (1.2) with high order accuracy in both space and time. High order accuracy in space can in principle be obtained in a straightforward way by simply expanding the difference operators to wider forms. If the derivation is carried out such that for example $(bp_x)_x$ is written as $bp_{xx} + b_x p_x$, and b_x is a known function, then the form of the higher order approximation is particularly simple, since high order formulas

$$p_x = \sum_{j=1}^{r-1} D_0(I + \alpha_j h^{2j} D_+^j D_-^j)p + \mathcal{O}(h^q)\,,$$

$$p_{xx} = \sum_{j=1}^{r-1} D_+ D_-(I + \beta_j h^{2j} D_+^j D_-^j)p + \mathcal{O}(h^q)\,,$$

of order $q = 2r$ are well known. However, the stability and accuracy properties of this type of approximations are not optimal if $b_x \neq 0$, and we are going to use more compact methods. In the second order accurate case, they have the form $D_+\left(b_{j-1/2} D_- p_j\right)$, and this form can be generalized to higher order, even if the derivation is cumbersome.

The construction of higher approximations in time is more difficult. For this, there are two main requirements that are important: we must have stability for as large time step k as possible, and we don't want to store the solutions at too many levels. In Sections 2.1 and 3.1, we will consider methods that use only three time-levels. In order to approximate p_{tt} with order of accuracy higher than two, we need more than three levels, since the truncation error of the standard second order approximation contains derivatives of order four. However, by reducing these time-derivatives to lower order by using the differential equation, we can retain the three level structure. This idea goes back to Numerov [20, 21], who considered ordinary differential equations of the type

$$\frac{d^2p}{dt^2} = f(p,t)\,,$$

and used the relation $d^4p/dt^4 = d^2f/dt^2$ to eliminate the truncation error of the standard second order approximation. However, the resulting method is implicit, and we want to keep it explicit. The next step is then to carry out the differentiation of f and to use the differential equation once more. If f is the linear differential operator in space corresponding to the wave equation, the result is a new expression containing only space derivatives. This idea was used by Lax and Wendroff for first order systems in their important paper [19]. More recently, it has also been used for the second order wave equation by Cohen and Joly [4] and Tuomela [26]. These construction methods lead to approximations of arbitrarily high order in the case of constant coefficients, but for variable coefficients, the latter method is only second order accurate in time. Here, we will modify the method, such that it becomes fourth order accurate in both space and time. We will call this method *the time compact method.*

The procedure of transferring time derivatives occurring in the truncation error to space derivatives may be rather cumbersome. With time-dependent coefficients or nonlinear problems, it may even be impossible, since we don't have any expression for $\partial p/\partial t$. Furthermore, even for the wave equation with coefficients depending only on the space variables, the resulting method contains higher order derivatives of the functions a and b, and if these are not available, a new difficulty arises. To avoid this, we use the deferred correction principle in time. The standard second order method is used to compute an intermediate solution $\tilde{p}$. This one is then used to approximate the truncation error in both space and time. By a slight modification of the stability concept, the stability limit on the time-step k is kept the same as for the second order method.

For long time integration, the error of the second order solution may become too large to be useful for approximating higher derivatives. To improve the accuracy, the method can be restarted at regular intervals, and we will demonstrate that this is indeed a useful method.

The acoustic as well as the electromagnetic wave equations are obtained by differentiation of first order systems as demonstrated in Chapter 1. An alternative is of course to use these original first order systems as the basis for the numerical method, and this is the standard way in electromagnetics. The procedure of transferring time derivatives to space derivatives is simpler in this case. Furthermore, by using a staggered grid, we get a very compact scheme without any parasitic solutions. In Section 3.1, we will develop the time compact fourth order method for the first order system formulation, and prove that it is stable under the same condition as the second order accurate scheme. We will also apply the deferred correction principle in both space and time, just as for the wave equation in second order formulation. Here, we limit ourselves to the case of periodic boundary conditions, and use Fourier technique for investigation of stability. The non-periodic cases are challenging problems, where high order discretizations of the boundary conditions remain to be found.

2 The wave equation, second order formulation

We consider the one-dimensional case of (1.1):

$$p_{tt} = a\left(bp_x\right)_x \ , \tag{3.1}$$

with smoothly varying coefficients $a(x)$ and $b(x)$ and 2π-periodic solutions in the x-direction. In the acoustic wave equation, we have $a = -c^2\,\rho$ and $b = 1/\rho$.

We examine compact, higher order methods for this equation, and introduce a regular grid with step length h and k in the x-and t-direction respectively

$$(x_j, t_n) = (jh, nk)\,, \quad j = 1, 2, \dots\,, \quad n = 0, 1, \dots ..$$

The standard second order finite difference method for this is

$$\begin{aligned} \tilde{p}_j^{n+1} - 2\tilde{p}_j^n + \tilde{p}_j^{n-1} &= \lambda^2 a_j \Big(b_{j+1/2}\tilde{p}_{j+1}^n - \\ &\qquad - \left(b_{j+1/2} + b_{j-1/2}\right)\tilde{p}_j^n + b_{j-1/2}\tilde{p}_{j-1}^n \Big) + k^2 F_j^n \,, \\ \tilde{p}_j^0 &= f_j \,, \\ \tilde{p}_j^1 &= g_j \,. \end{aligned} \tag{3.2}$$

Based on Fourier analysis for frozen coefficients, we choose

$$\lambda = \frac{k}{h} < \frac{1}{\max\limits_j \sqrt{a_j b_{j-1/2}}} \tag{3.3}$$

for stability. (For a discussion on stability concepts and the method of freezing the coefficients, see e.g. [14].) The function f in the initial condition is given, but g is computed by a fourth order Taylor expansion using an initial condition on $p_t(x, 0)$. The derivatives $p_{tt},\ p_{ttt},\ p_{tttt}$ at $t = 0$ are obtained by using the differential equation (3.1).

The periodicity condition

$$p_j^n = p_{j+N}^n$$

makes it possible to limit the computation to the interval $0 \leqslant x \leqslant 2\pi$, i.e., $j = 1, 2, \dots, N$ with $N = 2\pi/h$.

We start with the case of constant coefficients

$$p_{tt} = p_{xx} + F \tag{3.4}$$

The standard second order finite difference method for this is

$$\begin{aligned} \tilde{p}_j^{n+1} - 2\tilde{p}_j^n + \tilde{p}_j^{n-1} &= \lambda^2(\tilde{p}_{j+1}^n - 2\tilde{p}_j^n + \tilde{p}_{j-1}^n) + k^2 F_j^n \,, \\ \tilde{p}_j^0 &= f_j \,, \\ \tilde{p}_j^1 &= g_j \,, \end{aligned} \tag{3.5}$$

where $\lambda = k/h < 1$ for stability.

2.1 Time compact scheme

We first define a method that is fourth order accurate in space and second order in time by eliminating the second order space error term in (3.5):

$$\begin{aligned} p_j^{n+1} - 2p_j^n + p_j^{n-1} = \lambda^2(p_{j+1}^n - 2p_j^n + p_{j-1}^n) - \\ - \frac{\lambda^2}{12}(p_{j+2}^n - 4p_{j+1}^n + 6p_j^n - 4p_{j-1}^n + p_{j-2}^n) + k^2 F_j^n \,. \end{aligned} \tag{3.6}$$

For this, we pay the price of a reduced maximum time step. The stability condition of the (4,2)-method (3.6) is easily obtained as

$$\lambda < \frac{\sqrt{3}}{2} \,. \tag{3.7}$$

To achieve fourth order accuracy also in time, we use the differential equation to transfer derivatives in time to derivatives in space, a generalization of the original Numerov method that was applied to systems of ODE. The method becomes

$$\begin{aligned} p_j^{n+1} - 2p_j^n + p_j^{n-1} = \lambda^2 \left(p_{j+1}^n - 2p_j^n + p_{j-1}^n\right) + \\ + \frac{\lambda^4 - \lambda^2}{12} \left(p_{j+2}^n - 4p_{j+1}^n + 6p_j^n - 4p_{j-1}^n + p_{j-2}^n\right) + k^2 F_j^n + \\ + \frac{k^4}{12}\Big((F_{xx})_j^n + (F_{tt})_j^n\Big) \,. \end{aligned} \tag{3.8}$$

For the scheme (3.8) we obtain the somewhat unusual effect, that by increasing the accuracy, we also relax the stability condition to the same one as we have for the standard second order scheme

$$\lambda < 1 \,. \tag{3.9}$$

The same principle can of course be applied to any order of accuracy. This has been done by e.g. Tuomela [26], also for the multi-dimensional case. In this case with constant coefficients, the stability condition is found to be (3.9) for any order of accuracy in one dimension.

For numerical experiments we have used

$$F(x,t) = (1-\alpha^2)\sin(x-\alpha t)\,,$$

which gives the solution

$$p(x,t) = \sin(x-\alpha t)$$

to (3.4). Figures 3.1–3.3 show the errors

$$\max_j \left|p(x_j,t_n) - p_j^n\right|$$

as functions of time for a zero right hand side. The second and fifth columns of Table 3.2 list the maximum error during the time period.

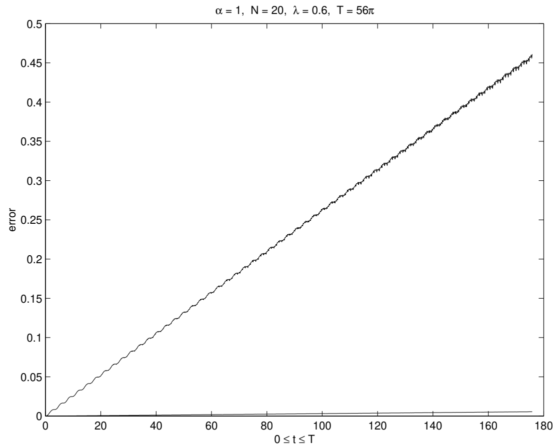

Figure 3.1: Error for 2nd order and 4th order time compact methods with $\alpha = 1$, $N = 20$, $\lambda = 0.6$, and $t \leqslant 56\pi$.

We now turn our attention to equation (3.1) with variable coefficients. For the related equation $p_{tt} = (\mu(x)p_x)_x$, Tuomela defines finite difference schemes that by construction are stable for $\lambda < 1$, but with only second order accuracy in time. We will give a (4,4)-method by using the differential equation. Cohen and Joly [4] has derived a similar, scheme that handles variable, and even irregular coefficients, by averaging them, and shown stability results. Their scheme is slightly more costly than the scheme described here, because of the more complicated evaluation of the coefficients.

To eliminate all second order truncation order terms in

$$D_+\left(\frac{1}{\rho_{j-1/2}}D_-p_j\right) = \left(\frac{1}{\rho}p_x\right)_x + \frac{h^2}{24}\left(\frac{1}{\rho}p_x\right)_{xxx} + \frac{h^2}{24}\left(\frac{1}{\rho}p_{xxx}\right)_x + \mathcal{O}(h^4)$$

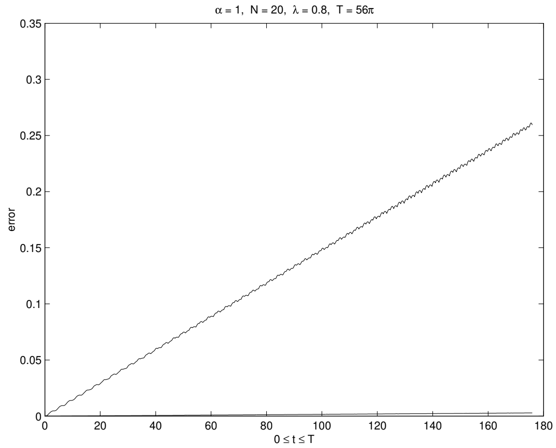

Figure 3.2: Error for 2nd order and 4th order time compact methods with $\alpha = 1$, $N = 20$, $\lambda = 0.8$, and $t \leqslant 56\pi$.

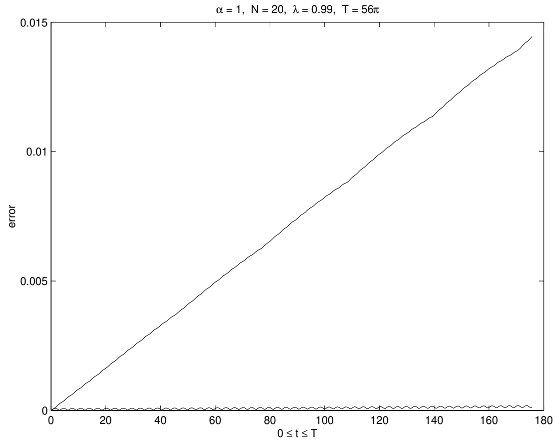

Figure 3.3: Error for 2nd order and 4th order time compact methods with $\alpha = 1$, $N = 20$, $\lambda = 0.99$, and $t \leqslant 56\pi$.

and

$$\frac{1}{c^2} D_+^t D_-^t p^n = \frac{1}{c^2} p_{tt} + \frac{1}{c^2} \frac{k^2}{12} p_{tttt} + \mathcal{O}(k^4)\,,$$

we use

$$\frac{1}{c^2} p_{tttt} = \rho \left(\frac{1}{\rho} \left(c^2 \rho \left(\frac{1}{\rho} p_x \right)_x \right)_x \right)_x - \frac{1}{\rho} \rho_x \left(c^2 F \right)_x + (c^2 F)_{xx} + F_{tt}$$

from (3.1) and obtain the scheme

$$
\begin{aligned}
\frac{1}{c_j^2}\frac{p_j^{n+1}-2p_j^n+p_j^{n-1}}{k^2} &= \rho_j D_+\left(\frac{1}{\rho_{j-1/2}}D_-p_j\right) - \\
&- \frac{h^2}{24}\rho_j D_+^2 D_-\left(\frac{1}{\rho_{j-1/2}}D_-p_j\right) - \frac{h^2}{24}\rho_j D_+\left(\frac{1}{\rho_{j-1/2}}D_+D_-^2p_j\right) + \\
&+ \frac{k^2}{12}\rho_j D_+\left(\frac{1}{\rho_{j-1/2}}D_-\left(c_j^2\rho_j D_+\left(\frac{1}{\rho_{j-1/2}}D_-p_j\right)\right)\right) + F_j + \\
&+ \frac{k^2}{12}\left(c_{xx,j}^2 - c_{x,j}^2\frac{1}{\rho_j}\rho_{x,j}\right)F_j + \frac{k^2}{12}\left(2c_{x,j}^2 - c_j^2\frac{1}{\rho_j}\rho_{x,j}\right)F_{x,j} + \\
&+ \frac{k^2}{12}\left(c_j^2F_{xx,j}+F_{tt,j}\right) + \mathcal{O}(k^4) + \mathcal{O}(k^2h^2) + \mathcal{O}(h^4)\,,
\end{aligned}
\tag{3.10}
$$

with

$$\lambda = \frac{k}{h} < \frac{1}{\max\limits_j |c|}$$

for stability.

Table 3.1 shows the error

$$\max_{j,n}\left|p(x_j,t_n)-p_j^n\right|$$

computed for $t \leqslant 8\pi$ (4 wavelengths) and $t \leqslant 56\pi$ (28 wavelengths) for the second order scheme and for the time compact fourth order scheme with $\alpha = 1$, $c^2(x) = (\sin(x)+2)/2$ and $\rho(x) = (\sin(x)+2)^{-1}$.

		$t \leqslant 8\pi$		$t \leqslant 56\pi$	
$\lambda \cdot c_{\max}$	N	$q=2$	$q=4$	$q=2$	$q=4$
	10	1.38	0.0061	9.7	0.012
0.6	20	0.37	0.00042	2.6	0.00074
	40	0.093	0.000027	0.65	0.000046
	10	3.3	0.0039	9.4	0.0072
0.8	20	0.34	0.00021	2.4	0.00044
	40	0.087	0.000014	0.61	0.000027
	10	1.3	0.0036	9.4	0.0051
0.99	20	0.31	0.00020	2.2	0.00030
	40	0.08	0.000012	0.55	0.000019

Table 3.1: The error in the case of variable coefficients for different values of λ.

2.2 Deferred correction

The truncation errors in time and space for (3.5) are $p_{tttt}/12$ and $p_{xxxx}/12$, respectively. The basic deferred correction method is obtained by first solving (3.5), and then eliminating the 2nd order truncation errors in both space and time in the second stage

$$
\begin{aligned}
p_j^{n+1} - 2p_j^n + p_j^{n-1} &= \lambda^2(p_{j+1}^n - 2p_j^n + p_{j-1}^n) + \\
&+ \frac{1}{12}(\tilde{p}_j^{n+2} - 4\tilde{p}_j^{n+1} + 6\tilde{p}_j^n - 4\tilde{p}_j^{n-1} + \tilde{p}_j^{n-2}) - \\
&- \frac{\lambda^2}{12}(\tilde{p}_{j+2}^n - 4\tilde{p}_{j+1}^n + 6\tilde{p}_j^n - 4\tilde{p}_{j-1}^n + \tilde{p}_{j-2}^n) + k^2 F_j^n\,.
\end{aligned}
\tag{3.11}
$$

For each new time-level, the computation of the solution p requires that the 2nd order solution $\tilde{p}$ is stored at 4 time-levels. Furthermore, $\tilde{p}$ is required for $t < 0$ in order to start the computation of u. We define $\tilde{p}^{-1}$ by using the 2nd order method (3.5) backwards in time:

$$\tilde{p}_j^{-1} - 2\tilde{p}_j^0 + \tilde{p}_j^1 = \lambda^2(\tilde{p}_{j+1}^0 - 2\tilde{p}_j^0 + \tilde{p}_{j-1}^0) + k^2 F_j^0\,,$$

The third and the sixth columns of Table 3.2 show the error

$$\max_{j,n} |p(x_j, t_n) - p_j^n|$$

in a calculation with the same forcing function as before for $\alpha = 1$ and $t \leqslant 8\pi$ (4 wavelengths) and $t \leqslant 56\pi$ (28 wavelengths) for schemes of accuracy order $q = 4$. We note that the error becomes smaller with larger values of λ, and that the

		$t \leqslant 8\pi$			$t \leqslant 56\pi$		
λ	N	$q=2$	$q=4$ (tc)	$q=4$ (dc)	$q=2$	$q=4$ (tc)	$q=4$ (dc)
	10	0.26	0.012	0.033	1.60	0.087	1.55
0.6	20	0.066	0.00079	0.0022	0.46	0.0055	0.11
	40	0.017	0.000049	0.00014	0.12	0.00034	0.0067
	10	0.15	0.0066	0.011	1.01	0.046	0.53
0.8	20	0.037	0.00041	0.00075	0.26	0.0029	0.034
	40	0.0093	0.000026	0.000048	0.065	0.00018	0.0021
	10	0.0080	0.0013	0.0013	0.060	0.0031	0.0032
0.99	20	0.0021	0.000084	0.000082	0.014	0.00019	0.00019
	40	0.00051	0.0000051	0.0000050	0.0036	0.000012	0.000012

Table 3.2: The error for different values of λ when $\alpha = 1$. The time compact scheme is denoted by tc and deferred correction by dc.

two fourth order schemes have almost the same error for $\lambda = 0.99$ The reason is that for $\alpha = 1$ the forcing function is zero, and for the limit value $\lambda = 1$, the truncation errors $p_{tttt}/12$ and $\lambda^2 p_{xxxx}/12$ cancel each other. Actually, for this case, both computed solutions $\tilde{p}$ and p are exact if the initial data are exact.

Figures 3.4–3.6 show the errors as functions of time. For $\alpha = 1.5$, the forcing

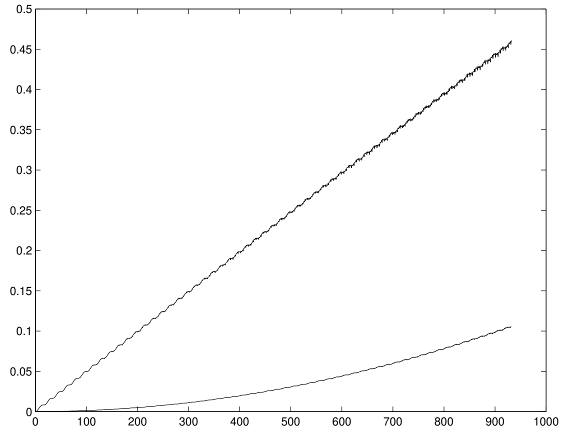

Figure 3.4: Error for 2nd order and 4th order deferred correction methods with $\alpha = 1$, $N = 20$, $\lambda = 0.6$, and $t \leqslant 56\pi$.

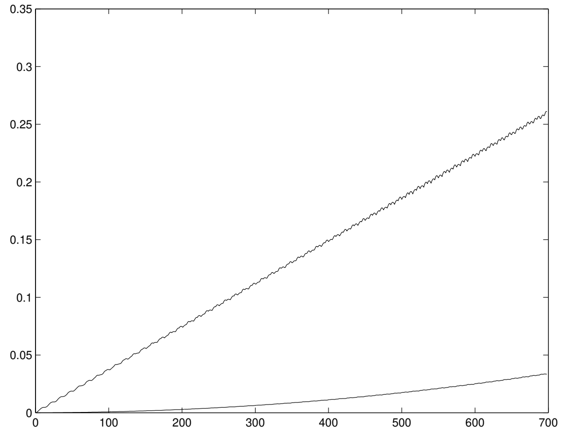

Figure 3.5: Error for 2nd order and 4th order deferred correction methods with $\alpha = 1$, $N = 20$, $\lambda = 0.8$, and $t \leqslant 56\pi$.

function is non-zero, and we get the errors shown in Table 3.3.

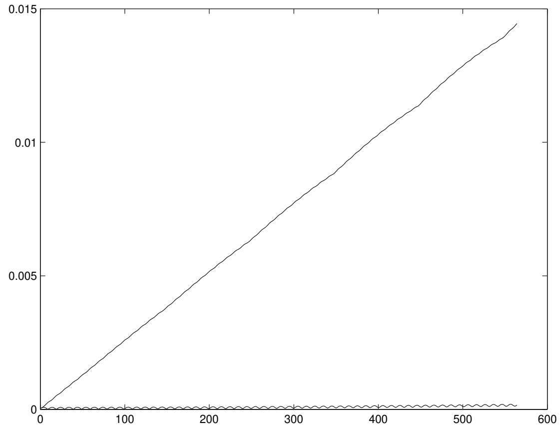

Figure 3.6: Error for 2nd order and 4th order deferred correction methods with $\alpha = 1$, $N = 20$, $\lambda = 0.99$, and $t \leqslant 56\pi$.

		$t \leqslant 8\pi$			$t \leqslant 56\pi$		
λ	N	$q = 2$	$q = 4$ (tc)	$q = 4$ (dc)	$q = 2$	$q = 4$ (tc)	$q = 4$ (dc)
	10	0.054	0.0026	0.0081	0.055	0.0026	0.059
0.6	20	0.013	0.00016	0.00052	0.014	0.00016	0.0037
	40	0.0032	0.000010	0.000033	0.0033	0.000010	0.00023
	10	0.15	0.0037	0.015	0.15	0.0037	0.094
0.8	20	0.036	0.00024	0.00095	0.037	0.00024	0.0058
	40	0.0088	0.000015	0.000058	0.0089	0.000015	0.00036
	10	0.27	0.0081	0.017	0.27	0.0081	0.021
0.99	20	0.063	0.00049	0.0010	0.063	0.00049	0.0013
	40	0.016	0.000030	0.000064	0.016	0.000030	0.000077

Table 3.3: The errors for different values of λ and $\alpha = 1.5$.

2.2.1 Restarted deferred correction

For long time integration, the error for any method increases, and finally it becomes unacceptable. This happens first for the lower order methods. The higher order solutions obtained by the deferred correction principle use the lower order ones as input, and if these have lost most of its accuracy, one cannot expect very accurate high order ones either. One possibility to improve this situation is to restart the method at regular intervals [7]. Such a restart at $t = \tau$ means that we redefine the second order solution $\tilde{p}$ by letting it take the values from the fourth order solution p at $t = \tau$ and $t = \tau + k$. To keep the smoothness, we recompute $\tilde{p}$ at $t = \tau - k$ by stepping backwards just like we do for starting the computation at $t = 0$. The results for restart at $\tau, 2\tau, \ldots$ are shown in Figures 3.7–3.9 for $\tau = 100k$.

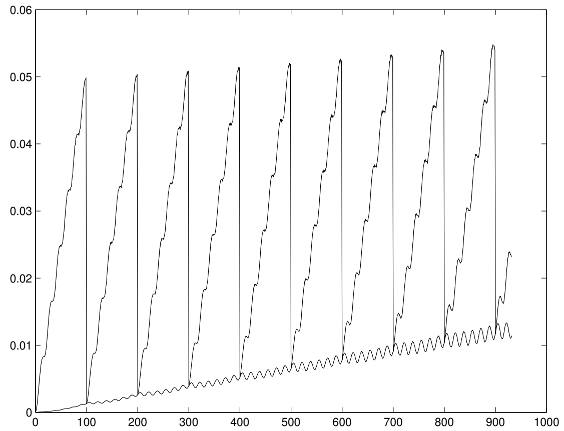

Figure 3.7: Error for 2nd order and 4th order restarted deferred correction methods with $\alpha = 1$, $N = 20$, $\lambda = 0.6$, $t \leqslant 56\pi$, and $\tau = 100k$.

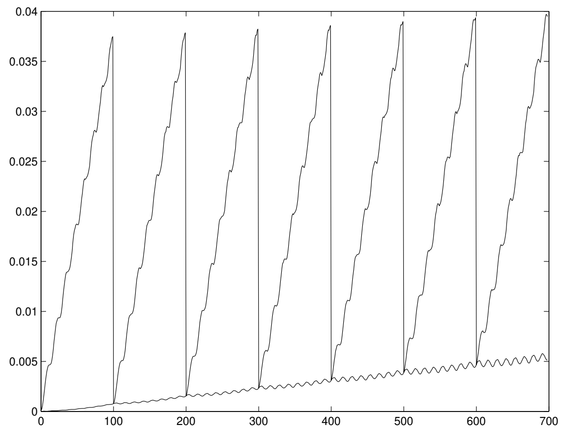

Figure 3.8: Error for 2nd order and 4th order restarted deferred correction methods with $\alpha = 1$, $N = 20$, $\lambda = 0.8$, $t \leqslant 56\pi$, and $\tau = 100k$.

These results indicate that the error in the fourth order solution is decreased by a factor that approximately equals the number of restarts r. However, there is a limit on r that is lower than T/k. The reason is that the stability analysis

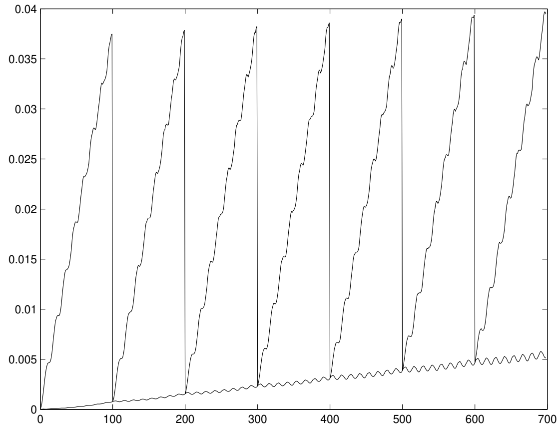

Figure 3.9: Error for 2nd order and 4th order restarted deferred correction methods with $\alpha = 1$, $N = 20$, $\lambda = 0.99$, $t \leqslant 56\pi$, and $\tau = 100k$.

does not hold uniformly in r, and our experiments indicate that r should be at most of order 10 before instabilities are triggered.

3 The wave equation in first order form

We now return to the wave equation in first order form (1.2). In one space dimension, this is written

$$\begin{bmatrix} p \\ u \end{bmatrix}_t = \begin{bmatrix} 0 & a(x) \\ b(x) & 0 \end{bmatrix} \begin{bmatrix} p \\ u \end{bmatrix}_x + \begin{bmatrix} F \\ G \end{bmatrix}, \quad t \geqslant 0, \tag{3.12}$$

with 2π-periodic solutions in the x-direction. The functions a and b are real and have the same sign. For the acoustic case, we have

$$\begin{aligned} a(x) &= c^2(x)\,\rho(x)\,, \\ b(x) &= 1/\rho(x)\,. \end{aligned}$$

With the notation $\mathbf{P} = (p,u)^T$, $\mathbf{F} = (F,G)^T$, we define the scalar product and the norm for vector functions by

$$(\mathbf{P}^{(1)}, \mathbf{P}^{(2)}) = \langle p^{(1)}, \frac{1}{|a|} p^{(2)} \rangle + \langle u^{(1)}, \frac{1}{|b|} u^{(2)} \rangle\,, \quad \|\mathbf{P}\|^2 = (\mathbf{P}, \mathbf{P})\,, \tag{3.13}$$

where the scalar product between scalar functions f, g is the usual one:

$$\langle f, g \rangle = \int_0^{2\pi} f(x) g(x) dx\,.$$

The solutions of the system (3.12) satisfy

$$\|\mathbf{P}\|\frac{d}{dt}\|\mathbf{P}\| = \frac{1}{2}\frac{d}{dt}\|\mathbf{P}\|^2 = (\mathbf{P},\mathbf{P}_t) = \langle p, \frac{1}{|a|}p_t\rangle + \langle u, \frac{1}{|b|}u_t\rangle + (\mathbf{P},\mathbf{F}) =$$
$$= \mathrm{sign}(a)(\langle p, u_x\rangle + \langle u, p_x\rangle) + (\mathbf{P},\mathbf{F}) = (\mathbf{P},\mathbf{F}) \leqslant \|\mathbf{P}\|\cdot\|\mathbf{F}\|\,.$$

After dividing by $\|\mathbf{P}\|$ and integrating with respect to t, we get

$$\|\mathbf{P}(\cdot,t)\| \leqslant \|\mathbf{P}(\cdot,0)\| + \int_0^t \|\mathbf{F}(\cdot,\tau)\| d\tau\,. \tag{3.14}$$

For the homogeneous case $\mathbf{F}=0$ we have $\|\mathbf{P}(\cdot,t)\| = \|\mathbf{P}(\cdot,0)\|$, i.e., the system is norm-conserving.

For the numerical solution, we introduce a staggered grid in space with step-length h, and in time with step-length k, such that u is stored at the middle points between p both in space and time:

$$p^{n+1/2}_{j+1/2} = p((j+1/2)h, (n+1/2)k)\,,$$
$$u^n_j = u(jh, nk)\,.$$

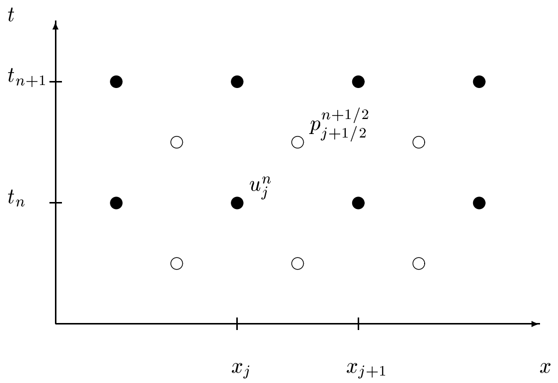

Figure 3.10: The unknowns are staggered in space and in time.

The well known second order method is

$$\begin{aligned} \tilde{p}^{n+1/2}_{j+1/2} &= \tilde{p}^{n-1/2}_{j+1/2} + ka_{j+1/2}D_+\tilde{u}^n_j + kF^n_{j+1/2}\,, \\ \tilde{u}^{n+1}_j &= \tilde{u}^n_j + kb_jD_-\tilde{p}^{n+1/2}_{j+1/2} + kG^{n+1/2}_j\,, \end{aligned} \tag{3.15}$$

where

$$\lambda = \frac{k}{h} \leqslant \frac{1}{\max\limits_j \sqrt{a_{j+1/2}b_j}} \tag{3.16}$$

for stability.

Let the discrete vector function $\mathbf{P}_j$ be defined by $\mathbf{P}_j = (p_{j+1/2}\ u_j)^T$, and consider the discrete operator Q_2 approximating the right hand side for $F = G = 0$ in (3.15):

$$Q_2\mathbf{P}_j = \begin{bmatrix} 0 & a_{j+1/2}D_+ \\ b_jD_- & 0 \end{bmatrix} \begin{bmatrix} p_{j+1/2} \\ u_j \end{bmatrix}, \quad j = 1, 2, \ldots, N\,.$$

Let the discrete scalar product be defined by

$$(\mathbf{P}^{(1)}, \mathbf{P}^{(2)})_h = \sum_{j=1}^{N} \left(\frac{1}{|a_{j+1/2}|} p^{(1)}_{j+1/2} p^{(2)}_{j+1/2} + \frac{1}{|b_j|} u^{(1)}_j u^{(2)}_j \right) h\,.$$

Without restriction we can assume that $a(x)$ and $b(x)$ are positive, and we have, by using summation by parts and the periodicity condition

$$\begin{aligned}(\mathbf{P}, Q_2\mathbf{P})_h &= \sum_{j=1}^{N} (p_{j+1/2}D_+u_j + u_jD_-p_{j+1/2})h \\ &= \sum_{j=1}^{N} (p_{j+1/2}D_+u_j - (D_+u_j)p_{j+1/2})h = 0\,,\end{aligned}$$

i.e., the discrete analogy of $(\mathbf{P}, \mathbf{P}_t) = 0$ is exactly preserved.

3.1 Time compact scheme

As for the scalar second order wave equation, we will derive the time compact method for the first order system. The fourth order version requires the elimination of the second order truncation errors both in space and time. The truncation error in space is $ah^2u_{xxx}/24$ for the p-equation, and $bh^2p_{xxx}/24$ for the u-equation. By differentiation of the system (3.12), we get

$$\begin{aligned}p_{ttt} &= a\,(b\,(au_x)_x)_x + a\,(bF_x)_x + aG_{xt} + F_{tt}\,, \\ u_{ttt} &= b\,(a\,(bp_x)_x)_x + b\,(aG_x)_x + bF_{xt} + G_{tt}\,.\end{aligned}$$

This leads to the fourth order scheme

$$
\begin{aligned}
p_{j+1/2}^{n+1/2} &= p_{j+1/2}^{n-1/2} + ka_{j+1/2}D_+u_j^n + \\
&+ \frac{k}{24}a_{j+1/2}(k^2D_+b_jD_-a_{j+1/2}D_+ - h^2D_+^2D_-)u_j^n + \\
&+ kF_{j+1/2}^n + \frac{k^3}{24}\Big((a(bF_x)_x)_{j+1/2}^n + (aG_{xt})_{j+1/2}^n + (F_{tt})_{j+1/2}^n\Big)\,, \\
u_j^{n+1} &= u_j^n + kb_jD_-p_{j+1/2}^{n+1/2} + \\
&+ \frac{k}{24}b_j(k^2D_-a_{j+1/2}D_+b_jD_- - h^2D_+D_-^2)p_{j+1/2}^{n+1/2} + \\
&+ kG_j^{n+1/2} + \frac{k^3}{24}\Big((b(aG_x)_x)_j^{n+1/2} + (bF_{xt})_j^{n+1/2} + (G_{tt})_j^{n+1/2}\Big)\,.
\end{aligned}
\tag{3.17}
$$

In analogy with the second order approximation, we define the fourth order difference operator Q_4 by

$$
Q_4\mathbf{P} = \begin{bmatrix} a_{j+1/2}D_+u_j^n + \dfrac{k^2}{24}a_{j+1/2}D_+b_jD_-a_{j+1/2}D_+u_j^n - \dfrac{h^2}{24}a_{j+1/2}D_+^2D_-u_j^n \\ \\ b_jD_-p_{j+1/2} + \dfrac{k^2}{24}b_jD_-a_{j+1/2}D_+b_jD_-p_{j+1/2} - \dfrac{h^2}{24}b_jD_+D_-^2p_{j+1/2} \end{bmatrix}.
$$

We use the same scalar product as above, and assume again without restriction that $a(x)$ and $b(x)$ are positive. We take the scalar product with $\mathbf{P}_j$, use summation by parts and the periodicity condition. Each element on the right hand side of the expression above consists of three terms. After summation by parts, the first term of the upper element cancels the first term of the lower element as shown for the second order scheme above. For the second term of the first element we have, when taking into account that the factor $a_{j+1/2}$ is canceled by the factor $1/a_{j+1/2}$ in the scalar product,

$$
\begin{aligned}
\sum_{j=1}^{N} p_{j+1/2}D_+b_jD_-a_{j+1/2}D_+u_jh &= -\sum_{j=1}^{N}(D_-p_{j+1/2})b_jD_-a_{j+1/2}D_+u_jh \\
&= \sum_{j=1}^{N}(D_+b_jD_-p_{j+1/2})a_{j+1/2}D_+u_jh \\
&= -\sum_{j=1}^{N}(D_-a_{j+1/2}D_+b_jD_-p_{j+1/2})u_jh\,.
\end{aligned}
$$

But the last expression is exactly the negative of the one obtained from the second term of the lower element when taking the scalar product, so they cancel each other. For the third term we have similarly

$$
\sum_{j=1}^{N} p_{j+1/2}D_+^2D_-u_jh = -\sum_{j=1}^{N}(D_-^2D_+p_{j+1/2})u_jh\,,
$$

which shows that also the third terms cancel each other in the scalar product. The conclusion is that our fourth order accurate difference operator has the same nice conservation property as the original differential operator, i.e.,

$$(\mathbf{P}, Q_4\mathbf{P})_h = 0\,.$$

The fully discrete approximation, where we discretize also in time, does not possess the conservation property exactly, but very closely. Figure 3.11 shows the norm

$$\sum_{j=1}^{N}\left(\frac{1}{|a_{j+1/2}|}p_{j+1/2}^2 + \frac{1}{|b_j|}u_j^2\right)h \tag{3.18}$$

as a function of time for the case $\alpha = 1$.

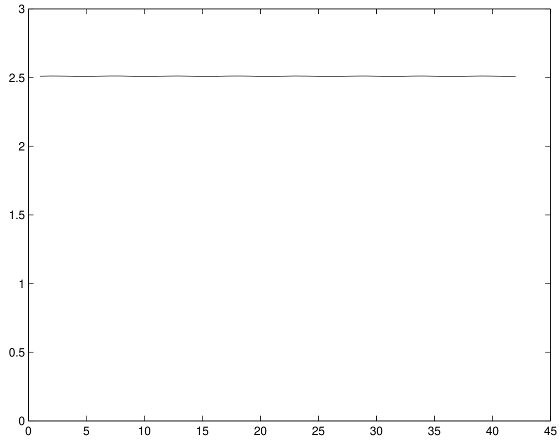

Figure 3.11: The norm (3.18) as a function of time, $\alpha = 1$, $N = 10$, $\lambda = 0.99$, and $t \leqslant 56\pi$.

For the stability analysis, we assume constant coefficients, and for convenience we let $a(x) = b(x) = -1$. By defining

$$p_{j+1/2}^{n-1/2} = \hat{p}^n e^{i\omega(j+1/2)h}\,,$$
$$u_j^n = \hat{u}^n e^{i\omega jh}\,,$$

we get the Fourier transformed system for the homogeneous case

$$\begin{bmatrix}\hat{p}^{n+1}\\ \hat{u}^{n+1}\end{bmatrix} = \begin{bmatrix}1 & \hat{Q}_q\\ \hat{Q}_q & 1+\hat{Q}_q^2\end{bmatrix}\begin{bmatrix}\hat{p}^n\\ \hat{u}^n\end{bmatrix},$$

where

$$\hat{Q}_2 = -2\lambda i \sin\frac{\xi}{2}\,,$$
$$\hat{Q}_4 = -2\lambda i \sin\frac{\xi}{2} - \frac{\lambda-\lambda^3}{3} i \sin^3\frac{\xi}{2}\,.$$

The eigenvalues μ of the amplification matrix are given by

$$\mu^2 - (2+\hat{Q}_q^2)\mu + 1 = 0\,.$$

Since $\hat{Q}_q^2$ is real and non-positive, the stability condition is $\hat{Q}_q^2 \geqslant -4$, i.e., $|\hat{Q}_q| \leqslant 2$. For $q=2$, we have the standard condition $\lambda \leqslant 1$. For $q=4$, we first assume that the same condition $\lambda \leqslant 1$ is satisfied, and obtain

$$\max_{0\leqslant\lambda\leqslant 1}\big(\max_{0\leqslant|\xi|\leqslant\pi} |\hat{Q}_4(\lambda,\xi)|\big) = \max_{0\leqslant\lambda\leqslant 1} |\hat{Q}_4(\lambda,\pi)| = \max_{0\leqslant\lambda\leqslant 1} 2\lambda\Big(1+\frac{1-\lambda^2}{6}\Big) = 2$$

for $\lambda = 1$. Obviously, $|\hat{Q}_4|$ has a positive slope at $\lambda=1$, showing that λ cannot be increased further without violating the stability.

The result shows that in accordance with the scalar wave equation case, the stability condition is not further restricted when going to fourth order accuracy using the time compact approach. This is in contrast to the (4,2) scheme, where only the truncation error in space is eliminated, such that the order of accuracy is four in space and two in time. In this case the factor $(\lambda-\lambda^3)/3$ in $\hat{Q}_4$ is substituted by $\lambda/3$, and we get the stability condition $\lambda \leqslant 6/7$.

The numerical experiments include one test with constant coefficients a and b, and one with variable coefficients. In the first case, we have used $a=b=1$ (note that these positive values correspond to the variable change $u \to -u$). The forcing functions are

$$F(x,t) = (1-\alpha^2)\sin(x-\alpha t)\,,$$
$$G(x,t) = 0\,,$$

which gives the solution

$$p(x,t) = -\alpha\cos(x-\alpha t)\,,$$
$$u(x,t) = \cos(x-\alpha t)\,.$$

The difference scheme requires differentiated forms of the forcing functions, and for convenience we list them here:

$$\begin{aligned}
a(bF_x)_x &= (\alpha^2-1)\sin(x-\alpha t)\,,\\
aG_{xt} &= 0\,,\\
F_{tt} &= \alpha^2(\alpha^2-1)\sin(x-\alpha t)\,,\\
b(aG_x)_x &= 0\,,\\
bF_{xt} &= (1-\alpha^2)\sin(x-\alpha t)\,,\\
G_{tt} &= 0\,.
\end{aligned}$$

The error is measured in the max-norm over space and time:

$$\max_{j,n}\left(|p(x_{j+1/2},t_{n+1/2})-p_{j+1/2}^{n+1/2}|,|u(x_j,t_n)-u_j^n|\right) .$$

The error is shown for two different values of T, in Table 3.4 for $\alpha = 1$ and in Table 3.5 for $\alpha = 1.5$.

λ	N	$t \leqslant 8\pi$	$t \leqslant 56\pi$
	10	0.017	0.12
0.2	20	0.0011	0.0076
	40	0.000068	0.00048
	10	0.014	0.10
0.4	20	0.00094	0.0066
	40	0.000059	0.00041
	10	0.011	0.078
0.6	20	0.00070	0.0049
	40	0.000044	0.00031
	10	0.00059	0.043
0.8	20	0.00038	0.0027
	40	0.000024	0.00017
	10	0.00033	0.0023
0.99	20	0.000020	0.00014
	40	0.0000013	0.0000090

Table 3.4: First order form, constant coefficients. The error for $\alpha = 1$.

In the second case with variable coefficients, we have used the forcing functions

$$F = (a(x) - \alpha^2)\sin(x - \alpha t) ,$$
$$G = \alpha(1 - b(x))\sin(x - \alpha t) ,$$

which gives the same solution as for the constant coefficient case. The coefficients are

$$a(x) = 1 + \varepsilon\sin(x) ,$$
$$b(x) = 1 ,$$

where $0 < \varepsilon < 1$. The wave speed is $c = \sqrt{1+\varepsilon\sin x}$, with the maximum wave speed $c_{max} = \sqrt{1+\varepsilon}$.

λ	N	$t \leqslant 8\pi$	$t \leqslant 56\pi$
	10	0.0036	0.0036
0.2	20	0.00023	0.00023
	40	0.000014	0.000014
	10	0.0032	0.0032
0.4	20	0.00020	0.00020
	40	0.000012	0.000012
	10	0.0027	0.0027
0.6	20	0.00017	0.00017
	40	0.000010	0.000010
	10	0.0024	0.0024
0.8	20	0.00015	0.00015
	40	0.0000091	0.0000091
	10	0.0030	0.0030
0.99	20	0.00018	0.00018
	40	0.000011	0.000011

Table 3.5: First order form, constant coefficients. The error for $\alpha = 1.5$.

The differentiated forms of the forcing functions are in this case

$$\begin{aligned}
a(bF_x)_x &= (1+\varepsilon\sin x)((\alpha^2 - 1 - 2\varepsilon\sin x)\sin(x-\alpha t) + 2\varepsilon\cos x\cos(x-\alpha t))\,,\\
aG_{xt} &= 0\,,\\
F_{tt} &= \alpha^2(\alpha^2 - 1 - \varepsilon\sin x)\sin(x-\alpha t)\,,\\
b(aG_x)_x &= 0\,,\\
bF_{xt} &= \alpha((1+\varepsilon\sin x - \alpha^2)\sin(x-\alpha t) - \varepsilon\cos x\cos(x-\alpha t))\\
G_{tt} &= 0\,.
\end{aligned}$$

The error is shown for $\varepsilon = 0.1$ for two different values of T, in Table 3.6 for $\alpha = 1$ and in Table 3.7 for $\alpha = 1.5$.

3.1.1 Two space dimensions

The equations are in this case

$$\begin{bmatrix} p \\ u \\ v \end{bmatrix}_t = \begin{bmatrix} 0 & a(x,y) & 0 \\ b(x,y) & 0 & 0 \\ 0 & 0 & 0 \end{bmatrix} \begin{bmatrix} p \\ u \\ v \end{bmatrix}_x + \begin{bmatrix} 0 & 0 & a(x,y) \\ 0 & 0 & 0 \\ b(x,y) & 0 & 0 \end{bmatrix} \begin{bmatrix} p \\ u \\ v \end{bmatrix}_y + \begin{bmatrix} F \\ G \\ H \end{bmatrix}.$$

$\lambda \cdot c_{\max}$	N	$t \leqslant 8\pi$	$t \leqslant 56\pi$
	10	0.018	0.12
0.2	20	0.0011	0.0079
	40	0.000071	0.00050
	10	0.015	0.11
0.4	20	0.00098	0.0069
	40	0.000062	0.00043
	10	0.012	0.085
0.6	20	0.00076	0.0054
	40	0.000048	0.00034
	10	0.0076	0.053
0.8	20	0.00047	0.0033
	40	0.000029	0.00020
	10	0.0024	0.014
0.99	20	0.00014	0.00090
	40	0.0000088	0.000056

Table 3.6: Variable coefficients. The error for $\alpha = 1$.

In the acoustic case, the new variable v is the velocity component in the y-direction, and a and b are defined in analogy with the one-dimensional case. With p and u stored as above, we now add v at the same time-levels as u, but staggered in the (x, y)-plane as shown in Figure 3.12.

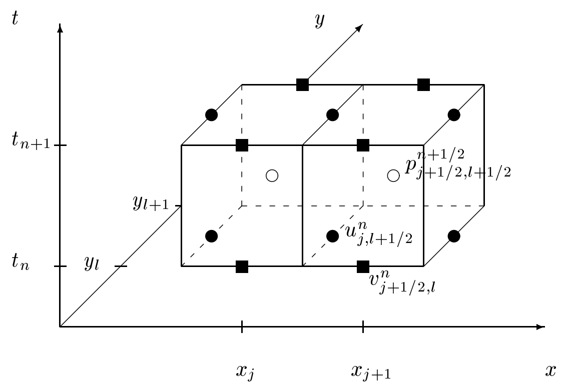

Figure 3.12: The unknowns u, v and p are staggered in space and in time.

$\lambda \cdot c_{\max}$	N	$t \leqslant 8\pi$	$t \leqslant 56\pi$
	10	0.0036	0.0036
0.2	20	0.00023	0.00023
	40	0.000014	0.000014
	10	0.0032	0.0033
0.4	20	0.00020	0.00020
	40	0.000013	0.000013
	10	0.0030	0.0030
0.6	20	0.00018	0.00018
	40	0.000011	0.000011
	10	0.0032	0.0032
0.8	20	0.00019	0.00019
	40	0.000012	0.000012
	10	0.0040	0.0041
0.99	20	0.00023	0.00023
	40	0.000014	0.000014

Table 3.7: Variable coefficients. The error for $\alpha = 1.5$.

The difference scheme is obtained as a direct generalization of the one-dimensional form. Here we limit ourselves to the constant coefficient case $a = b = -1$. Then the standard second order scheme is

$$\begin{aligned}
\tilde{p}^{n+1/2}_{j+1/2,\,l+1/2} &= \tilde{p}^{n-1/2}_{j+1/2,\,l+1/2} - \lambda_1(\tilde{u}^n_{j+1,\,l+1/2} - \tilde{u}^n_{j,\,l+1/2}) - \\
&\quad - \lambda_2(\tilde{v}^n_{j+1/2,\,l+1} - \tilde{u}^n_{j+1/2,\,l}) + kF^n_{j+1/2,\,l+1/2}\,, \\
\tilde{u}^{n+1}_{j,\,\nu} &= \tilde{u}^n_{j,\,\nu} - \lambda_1(\tilde{p}^{n+1/2}_{j+1/2,\,\nu} - \tilde{p}^{n+1/2}_{j-1/2,\,\nu}) + kG^{n+1/2}_{j,\,\nu}\ , \ \ \nu = l + 1/2\,, \\
\tilde{v}^{n+1}_{\nu,\,l} &= \tilde{v}^n_{\nu,\,l} - \lambda_2(\tilde{p}^{n+1/2}_{\nu,\,l+1/2} - \tilde{p}^{n+1/2}_{\nu,\,l-1/2}) + kH^{n+1/2}_{\nu,\,l}\ , \ \ \nu = j + 1/2\,,
\end{aligned}$$

where $\lambda_1 = k/h_1$, and $\lambda_2 = k/h_2$. The truncation errors in space are eliminated as in the one-dimensional case by approximating the third order derivatives by four-point formulas. For the truncation error in time, we use the relations

$$\begin{aligned}
p_{ttt} &= -u_{xxx} - u_{xyy} - v_{xxy} - v_{yyy} + F_{xx} + F_{yy} + F_{tt} - G_{xt} - H_{yt}\,, \\
u_{ttt} &= -p_{xxx} - p_{xyy} - F_{xt} + G_{xx} + G_{tt} + H_{xy}\,, \\
v_{ttt} &= -p_{yyy} - p_{xxy} - F_{yt} + G_{xy} + H_{yy} + H_{tt}\,,
\end{aligned}$$

and use second order accurate formulas for approximation of the space derivatives.

We omit writing down the complete fourth order approximation, and turn to the Fourier stability analysis. We define

$$\begin{aligned}
p^{n-1/2}_{j+1/2,l+1/2} &= \hat{p}^n e^{i\omega_1(j+1/2)h_1} e^{i\omega_2(l+1/2)h_2}\,,\\
u^n_{j,l+1/2} &= \hat{u}^n e^{i\omega_1 j h_1} e^{i\omega_2(l+1/2)h_2}\,,\\
v^n_{j+1/2,l} &= \hat{v}^n e^{i\omega_1(j+1/2)h_1} e^{i\omega_2 l h_2}\,,
\end{aligned}$$

and get for the homogeneous case

$$\begin{bmatrix} 1 & 0 & 0\\ -\hat{Q}_{q1} & 1 & 0\\ -\hat{Q}_{q2} & 0 & 1\end{bmatrix}\begin{bmatrix}\hat{p}^{n+1}\\ \hat{u}^{n+1}\\ \hat{v}^{n+1}\end{bmatrix} = \begin{bmatrix} 1 & \hat{Q}_{q1} & \hat{Q}_{q2}\\ 0 & 1 & 0\\ 0 & 0 & 1\end{bmatrix}\begin{bmatrix}\hat{p}^{n}\\ \hat{u}^{n}\\ \hat{v}^{n}\end{bmatrix}$$

i.e.,

$$\begin{bmatrix}\hat{p}^{n+1}\\ \hat{u}^{n+1}\\ \hat{v}^{n+1}\end{bmatrix} = \begin{bmatrix} 1 & \hat{Q}_{q1} & \hat{Q}_{q2}\\ \hat{Q}_{q1} & 1+\hat{Q}^2_{q1} & \hat{Q}_{q1}\hat{Q}_{q2}\\ \hat{Q}_{q2} & \hat{Q}_{q1}\hat{Q}_{q2} & 1+\hat{Q}^2_{q2}\end{bmatrix}\begin{bmatrix}\hat{p}^{n}\\ \hat{u}^{n}\\ \hat{v}^{n}\end{bmatrix}\,,\quad q = 2,4\,.$$

Here

$$\begin{aligned}
\hat{Q}_{2j} &= -2\lambda_j i \sin\frac{\xi_j}{2}\,,\quad j = 1,2\,,\\
\hat{Q}_{4j} &= -2\lambda_j i \sin\frac{\xi_j}{2} - \lambda_j(1-\lambda_j^2)\frac{i}{3}\sin^3\frac{\xi_j}{2}\,,\quad j = 1,2\,,
\end{aligned}$$

where $\hat{Q}_{qj}$ corresponds to the method of order q. One eigenvalue μ of the amplification matrix is one, the other two are defined by

$$(1-\mu)^2 - (\hat{Q}^2_{q1} + \hat{Q}^2_{q2})(1-\mu) - \hat{Q}^2_{q1}\hat{Q}^2_{q2} - \hat{Q}^2_{q1} - \hat{Q}^2_{q2} = 0\,.$$

It is easily shown that the stability condition becomes

$$\lambda_1 + \lambda_2 \leqslant 1 \tag{3.19}$$

for both cases $q = 2$ and $q = 4$. Hence, also for first order systems, the time compact fourth order scheme has the same stability limit as the standard second order scheme.

3.2 Deferred correction

The deferred correction method is obtained by first computing the solutions $\tilde{p}$ and $\tilde{u}$ of the second order accurate scheme (3.15), and then in the second stage using this solution for eliminating the truncation errors. The truncation error in space is as shown above for the time compact method, and the truncation error in time is $k^2 p_{ttt}/24$ and $k^2 u_{ttt}/24$. The fourth order approximation is

$$
\begin{aligned}
p_{j+1/2}^{n+1/2} &= p_{j+1/2}^{n-1/2} + k a_{j+1/2} D_+ u_j^n + \\
&+ \frac{k^3}{24}(\tilde{p}_{j+1/2}^{n+3/2} - 3\tilde{p}_{j+1/2}^{n+1/2} + 3\tilde{p}_{j+1/2}^{n-1/2} - \tilde{p}_{j+1/2}^{n-3/2}) - \\
&- \frac{kh^2}{24} a_{j+1/2} D_+^2 D_- \tilde{u}_j^n + kF_{j+1/2}^n \,, \\
u_j^{n+1} &= u_j^n + k b_j D_- p_{j+1/2}^{n+1/2} + \frac{k^3}{24}(\tilde{u}_j^{n+2} - 3\tilde{u}_j^{n+1} + 3\tilde{u}_j^n - \tilde{u}_j^{n-1}) - \\
&- \frac{kh^2}{24} b_j D_+ D_-^2 \tilde{p}_{j+1/2}^{n+1/2} + kG_j^{n+1/2} \,.
\end{aligned}
\tag{3.20}
$$

For each new time-level, the computation of the solution (p, u) requires that the 2nd order solution $(\tilde{p}, \tilde{u})$ is stored at four time-levels.

Since p is stored at half-points in time, we need $p^{1/2}$ to get started. This can be computed by using a one-step method, but we will assume that $p(x, k/2)$ is known. Furthermore, $(\tilde{p}, \tilde{u})$ is required for $t < 0$ in order to start the computation of (p, u). We define $(\tilde{p}^{-1/2}, \tilde{u}^{-1})$ by using the 2nd order method (3.15) backwards in time:

$$
\begin{aligned}
\tilde{p}_{j+1/2}^{-1/2} &= \tilde{p}_{j+1/2}^{1/2} - k a_{j+1/2} D_+ \tilde{u}_j^0 - kF_{j+1/2}^0 \,, \\
\tilde{u}_j^{-1} &= \tilde{u}_j^0 - k b_j D_- \tilde{p}_{j+1/2}^{-1/2} - kG_j^{-1/2} \,.
\end{aligned}
\tag{3.21}
$$

The stability properties of the deferred correction methods are determined by the basic second order method, in our case the scheme (3.15). In the second stage (3.20) of the algorithm, the solution $(\tilde{p}, \tilde{u})^T$ is considered as a forcing function, and the standard technique for estimation of the solution by using the Duhamel's principle is applied. This procedure was carried out for a scalar equation and an implicit method in [13], and the result is easily carried over to our case. Let

$$
\mathbf{P}^n = (p^{n+1/2}, u^n)^T \,, \mathbf{F}^n = (F^{n+1}, G^{n+1/2})^T \,,
$$

and let $\|\mathbf{P}\|_h$ be the discrete norm corresponding to (3.13). If the stability condition (3.16) is satisfied, then the solution of (3.20) satisfies the estimate

$$
||\mathbf{P}^n||_h \leqslant \mathrm{C}\left(\sum_{\mu=0}^{1}(||(D_+)^\mu \mathbf{P}^0||_h + \max_{0\leqslant\nu\leqslant n} ||(D_+)^\mu \mathbf{F}^\nu||_h) + \max_{0\leqslant\nu\leqslant n} ||D_+^t \mathbf{F}^{\nu+1/2}||_h\right) .
$$

For the numerical experiments we have used the same problem and the same error norm as in Section 3.1, i.e., the max-norm over space and time. The error is shown in Table 3.8.

	$t \leqslant 8\pi$		$t \leqslant 56\pi$	
N	$q=2$	$q=4$	$q=2$	$q=4$
10	0.22	0.0098	0.22	0.012
20	0.052	0.00060	0.052	0.00076
40	0.013	0.000037	0.013	0.000047

Table 3.8: The error in deferred correction method (3.20) for $\lambda = 0.99$.

4 Conclusions

We have defined several approaches to construct explicit finite difference schemes for the wave equation, that are fourth order accurate, not only in space, but also in time. The extension to even higher order methods are in principle straightforward, but perhaps a bit cumbersome for variable coefficients. First of all, we have a choice in the formulation of the problem. Either we can use the second order wave equation, or we can use a system of first order differential equations, preferably on a staggered grid to avoid parasitic solutions. For both cases, we have formulated a Numerov-type method and a deferred correction method and our numerical experiments confirm the accuracy and stability of the methods.

The error in the computed solution will grow with time. For applications where the total time is very long compared to the wavelength of the problem, a fourth order method may not be efficient enough. One way to proceed is to develop sixth order methods in the same way as done here for fourth order methods. For time-harmonic problems, an alternative is to work with the Helmholtz equation, as described in the previous chapters. This also has the advantage that boundary conditions easily can be discretized to preferred order of accuracy.

References

[1] R. F. Boisvert. Families of high order accurate discretizations of some elliptic problems. *SIAM J. Sci. Statist. Comput.*, 2:268–284, 1981.

[2] L. M. Brekhovskikh and O. A. Godin. *Acoustics of Layered Media I: Plane and Quasi-Plane Waves.* Springer-Verlag, Berlin, 1990.

[3] D. K. Cheng. *Field and Wave Electromagnetics.* Addison–Wesley, Reading, MA, 2nd edition, 1989.

[4] G. Cohen and P. Joly. Construction and analysis of fourth-order finite difference schemes for the acoustic wave equation in nonhomogeneous media. *SIAM J. Numer. Anal.*, 33:1266–1302, 1996.

[5] L. Collatz. *The Numerical Treatment of Differential equations.* Springer-Verlag, Berlin, 3rd edition, 1960.

[6] B. Engquist and A. Majda. Absorbing boundary conditions for the numerical simulation of waves. *Math. Comput.*, 31:629–651, 1977.

[7] B. Fornberg. Private communication.

[8] B. Fornberg. Calculation of weights in finite difference formulas. *SIAM Rev.*, 40:685–691, 1998.

[9] L. Fox. The numerical solution of elliptic differential equations when the boundary conditions involve a derivative. *Philos. Trans. Roy. Soc. London Ser. A*, 242:345–378, 1950.

[10] G. H. Golub and C. F. Van Loan. *Matrix Computations*, chapter 4.3. The Johns Hopkins University Press, Baltimore. MD, 3rd edition, 1996.

[11] B. Gustafsson and L. Hemmingsson-Frändén. A fast domain decomposition high order Poisson solver. *J. Sci. Comput.*, 14:223–243, 1999.

[12] B. Gustafsson and L. Hemmingsson-Frändén. Implicit high-order difference methods and domain decomposition for hyperbolic problems. *Appl. Numer. Math.*, 33:493–500, 2000.

[13] B. Gustafsson and L. Hemmingsson-Frändén. Deferred correction in space and time. *J. Sci. Comput.*, 16, 2001. To appear.

[14] B. Gustafsson, H.-O. Kreiss, and J. Oliger. *Time Dependent Problems and Difference Methods*, chapter 3. John Wiley & Sons, New York, 1995.

[15] B. Gustafsson and W. Kress. Deferred correction methods for initial value boundary value problems. *J. Sci. Comput.*, 16, 2001. To appear.

[16] B. Gustafsson and W. Kress. Deferred correction methods for initial value problems. *BIT*, 41:986–995, 2001.

[17] F. B. Jensen, W. A. Kuperman, M. B. Porter, and H. Schmidt. *Computational Ocean Acoustics.* AIP Press, New York, 1994.

[18] H.-O. Kreiss and J. Oliger. Comparison of accurate methods for the integration of hyperbolic equations. *Tellus*, 24:199–215, 1972.

[19] P. D. Lax and B. Wendroff. Difference schemes for hyperbolic equations with high order accuracy. *Comm. Pure Appl. Math.*, 17:381–398, 1964.

[20] B. V. Noumerov. A method of extrapolation of perturbations. *Monthly Notices Roy. Astronom. Soc.*, 84:592–601, 1924.

[21] B. Numerov. Note on the numerical integration of $d^2x/dt^2 = f(x,t)$. *Astronom. Nachr.*, 230:359–364, 1927.

[22] K. Otto. Iterative solution of the Helmholtz equation by a fourth-order method. *Boll. Geof. Teor. Appl.*, 40 suppl.:104–105, 1999.

[23] K. Otto and E. Larsson. Iterative solution of the Helmholtz equation by a second-order method. *SIAM J. Matrix Anal. Appl.*, 21:209–229, 1999.

[24] V. Pereyra. Accelerating the convergence of discretization algorithms. *SIAM J. Numer. Anal.*, 4:508–533, 1967.

[25] B. Swartz and B. Wendroff. The relative efficiency of finite difference and finite element methods. I: Hyperbolic problems and splines. *SIAM J. Numer. Anal.*, 11:979–993, 1974.

[26] J. Tuomela. On the construction of arbitrary order schemes for the many dimensional wave equation. *BIT*, 36:158–165, 1996.